

# Silicon Friendly Materials and Device Solutions for Microenergy Applications



[sinergy-project.eu](http://sinergy-project.eu)

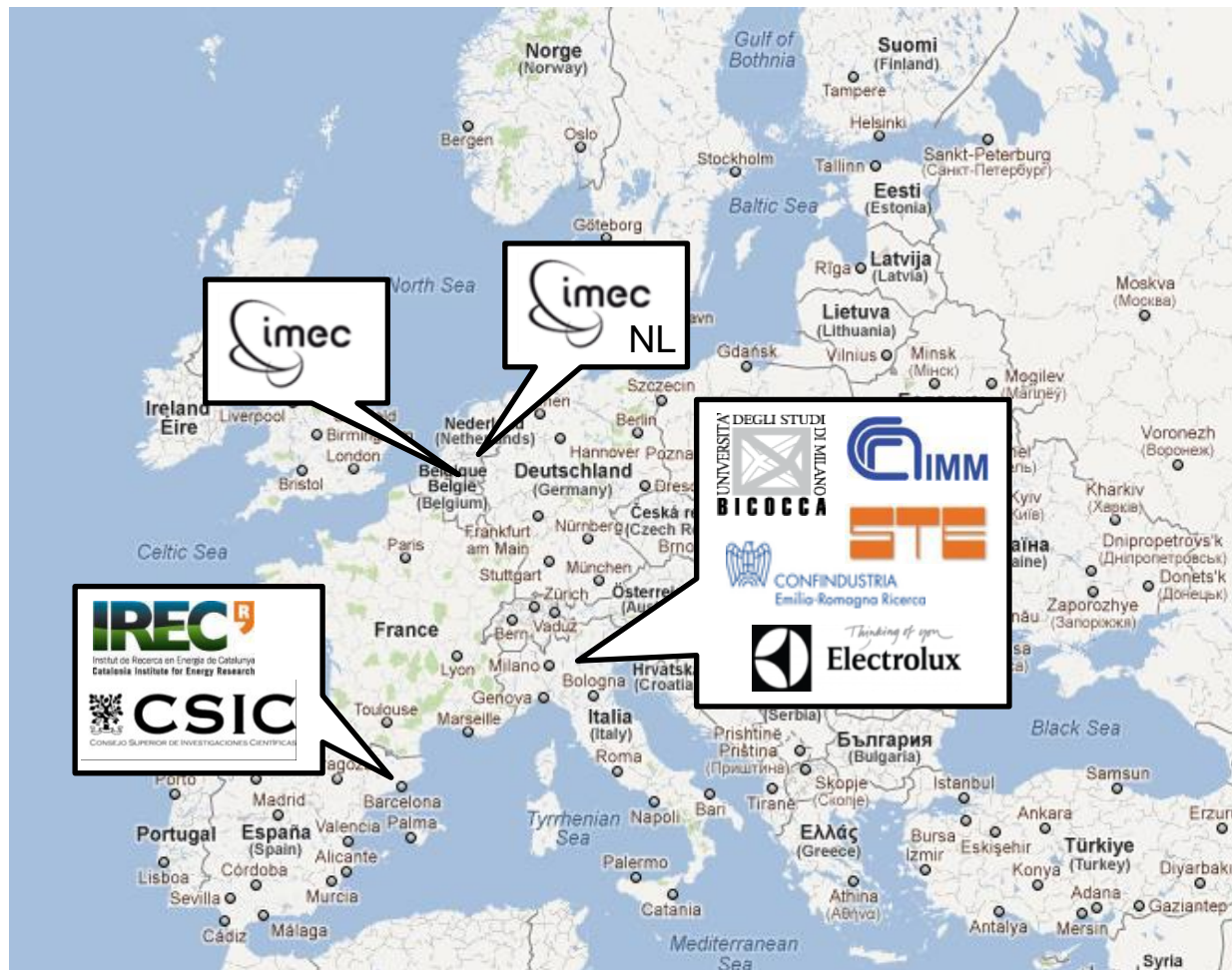
# Silicon as a Key Material for Multiphysics Microharvesting: the SiENERGY Project



Dario Narducci,  
Univ. of Milano Bicocca, Dept. Materials Science  
[dario.narducci@unimib.it](mailto:dario.narducci@unimib.it)

## Outline

- Why «all silicon»
- Demo applications
- Redundancy
- Thermoelectric generators:
  - bottom-up
  - top-down
- Mechanical harvesting:
  - electrostatic
  - vibrational
- Batteries
- Some conclusions



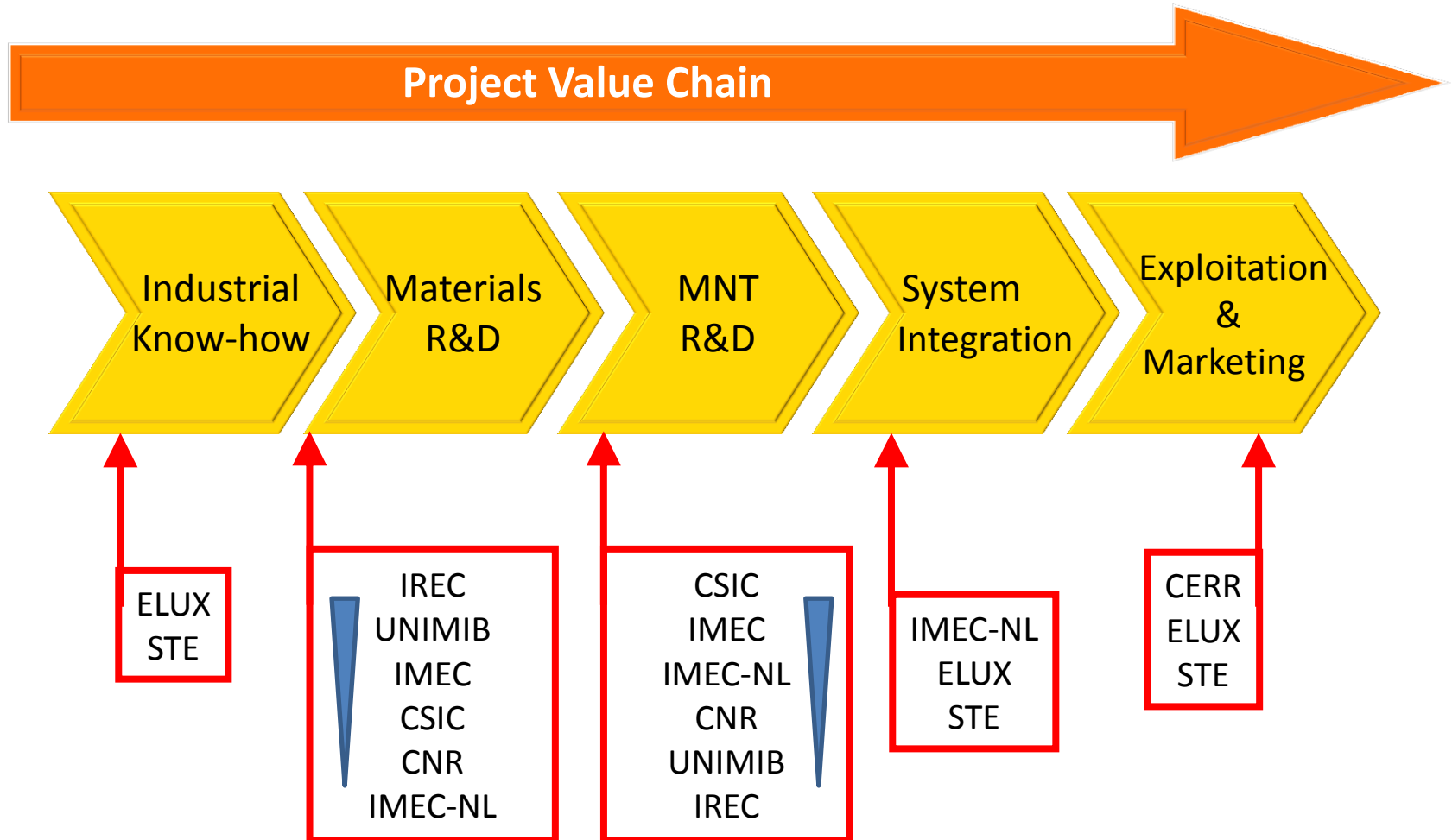
9 partners  
(E, I, BE, NL)

**Coordinator:**  
CSIC  
(IMB-CNM)

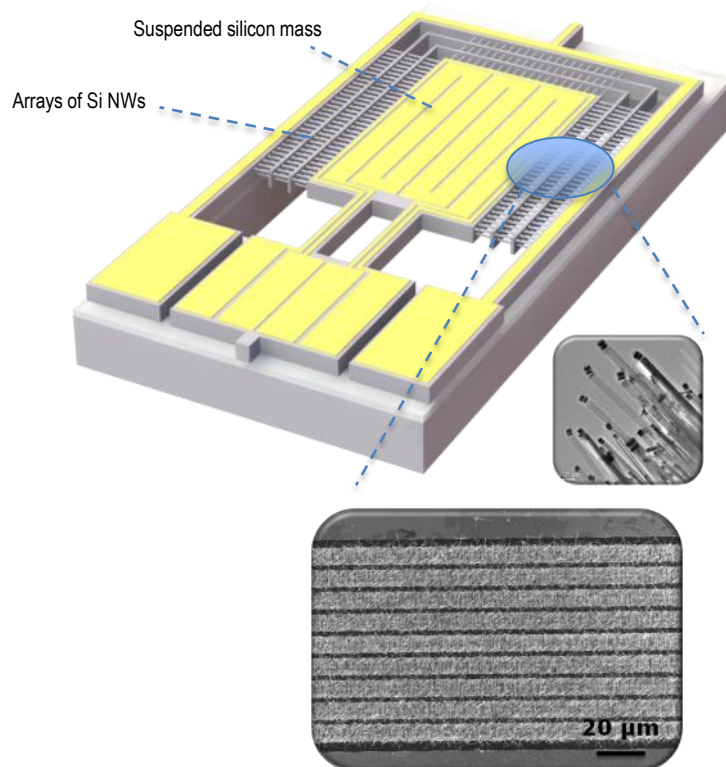
**Why microenergy solutions:** Replace primary batteries (cost, environmental, deployment flexibility issues) by harvesters + secondary batteries

**Why Silicon materials and architectures:** tap into the micro-nanoelectronics field which is an enabling technology, dealing with miniaturised and high density features (3D) implementations, offering economy of scale (serve mass markets) and the possibility of integration and addition of control and smartness

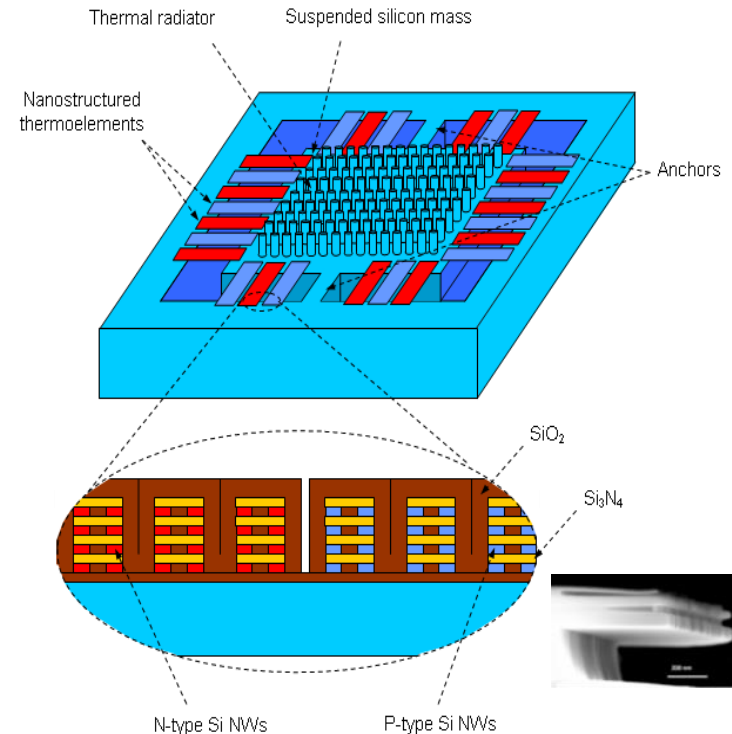
**Why such applications:** complementary microenergy testbeds from the perspective of silicon benefits ('smaller is better', 'cheaper is better') and availability of energy harvesting sources



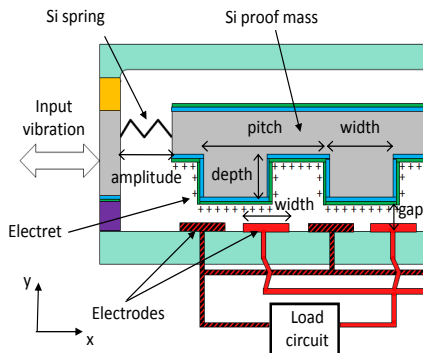
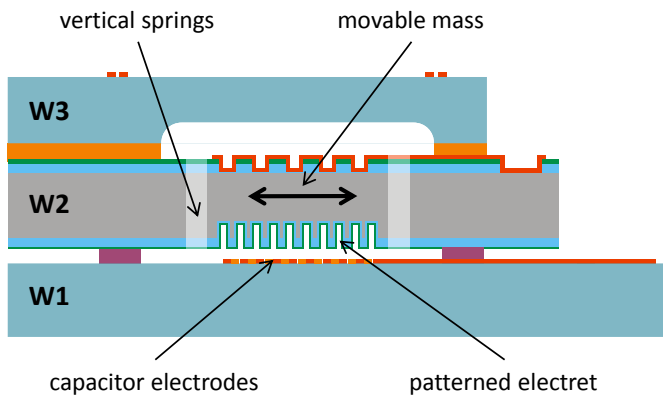
- 3D microstructures + bottom-up SiNWs



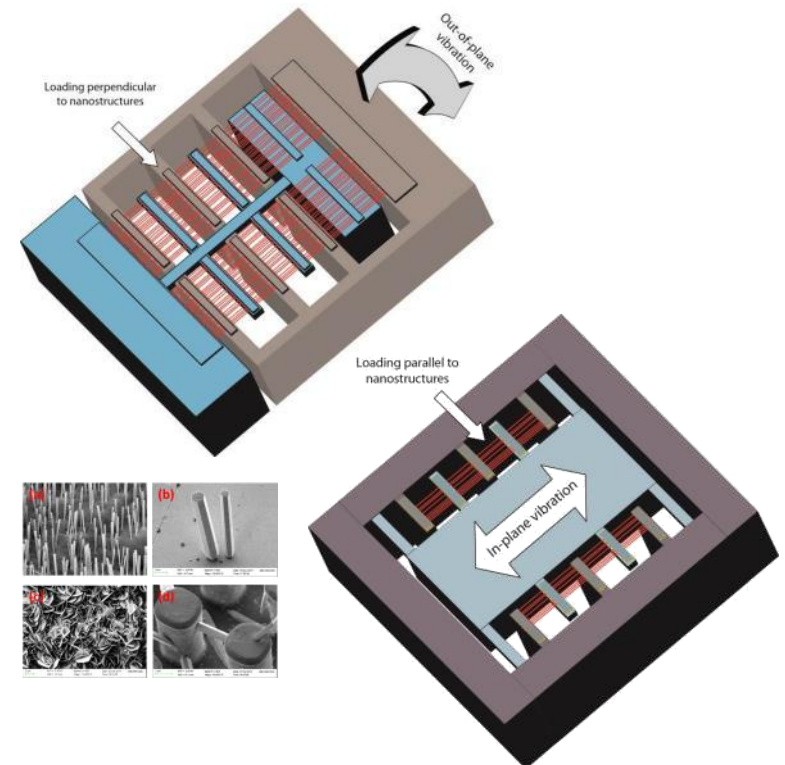
- 3D microstructures + top-down SiNWs



- 3D microstructures + electrostatic



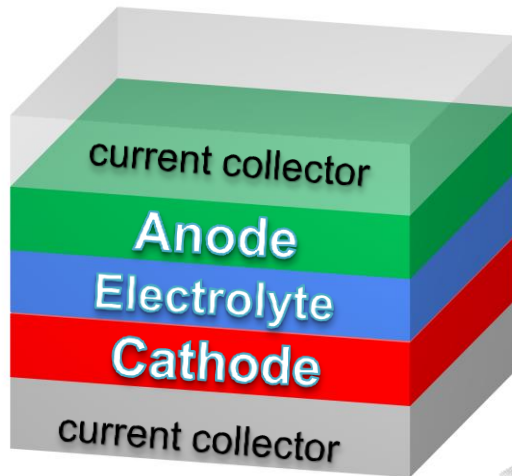
- 3D microstructures + piezoelectric





- Materials for Si compatible batteries

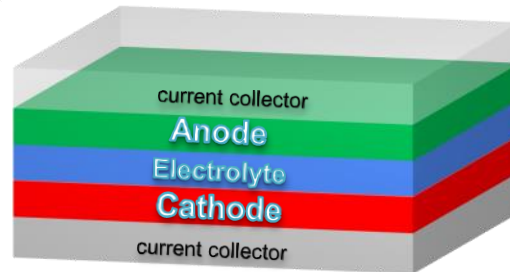
- 3D microstructures



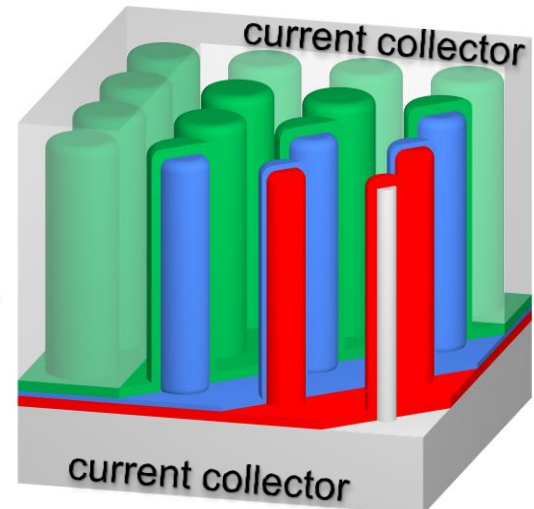
High capacity  
Low power

Thin film

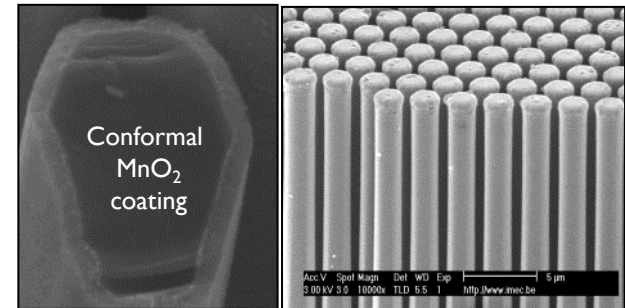
Low capacity  
High power



3D



High capacity & power



## Smart Pot



Cooking control

*High-value niche market*

*Portable and adaptive*

Test-bed for thermal harvesting

## Tire Pressure monitoring



Intelligent tire

*Large market volume*

*Small size*

Test-bed for vibration harvesting

## Predictive maintenance



Rotating-reciprocating machines

Large shop floors

*High number of nodes*

*Difficult servicing*

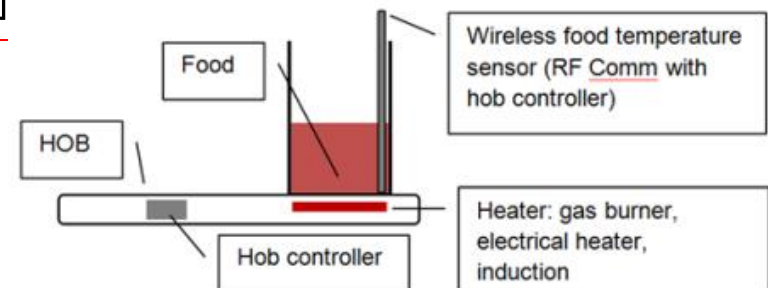
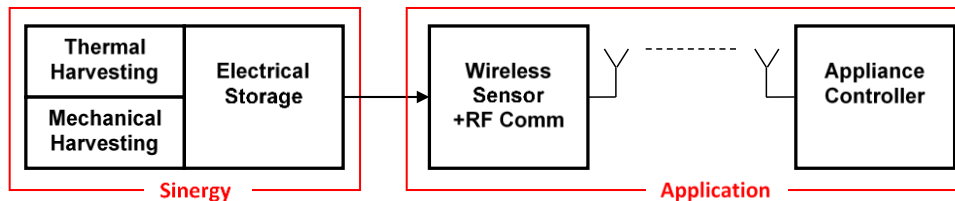
Test-bed for vibration and thermal harvesting

## Is technology at least potentially adequate?

- Predictive maintenance/domestic application system
  - Thermal harvester requirements under application conditions
  - Sensor system architecture
  - Planning/choice of application demonstrator
- Tire Pressure Monitoring Systems (TPMS)
  - Vibration harvester performance under application conditions
  - TPMS architecture
  - Planning

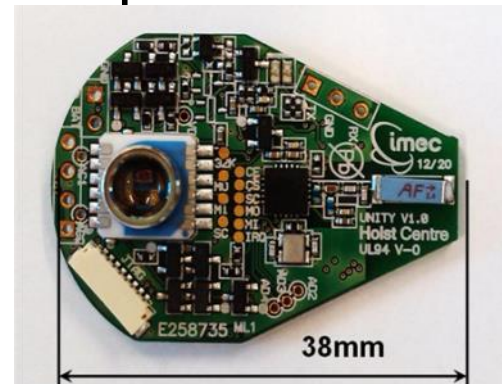
## Domestic appliances

- Food temperature in pots: 80-250 °C
- Transmit temperature to HOB



## Predictive maintenance

- Sensors: temperature, acceleration
- Reuse sensor system from IMEC and add new sensors (low power acceleration/temperature sensors) with programmable logic



- Preference is thermal energy harvester with off the shelf power management IC

- Machine guide values
  - displacements in the operational ranges 17.8 – 1125  $\mu\text{m}$  (rms);
  - velocity in the operational ranges 1.12 – 70.7 mm/s (rms);
  - acceleration in the operational ranges 1.76 – 111  $\text{m/s}^2$  (rms);
  - Temperature range: 10-60  $^{\circ}\text{C}$

Vibration severity grade	Maximum values of overall vibration measured on the machine structure			Machine vibration classification number						
	Displacement $\mu\text{m}$ (r.m.s.)	Velocity mm/s (r.m.s.)	Acceleration $\text{m/s}^2$ (r.m.s.)	1	2	3	4	5	6	7
				Evaluation zones						
1,1	17,8	1,12	1,76							
1,8	28,3	1,78	2,79	A/B						
2,8	44,8	2,82	4,42		A/B					
4,5	71,0	4,46	7,01			A/B				
7,1	113	7,07	11,1	C				A/B		
11	178	11,2	17,6		C				A/B	
18	283	17,8	27,9			C				
28	448	28,2	44,2				C			
45	710	44,6	70,1	D				C		
71	1125	70,7	111		D				C	
112	1784	112	176			D		D		C
180									D	D

Key to zones  
 A: The vibration of newly commissioned machines would normally fall within this zone  
 B: Machines with vibration within this zone are normally considered acceptable for long-term operation  
 C: Machines with vibration within this zone are normally considered unsatisfactory for long-term continuous operation. Generally, the machine may be operated for a limited period in this condition until a suitable opportunity arises for remedial action.  
 D: Vibration values within this zone are normally considered to be of sufficient severity to cause damage to the machine.

Table 2.8 Vibration classification numbers and guide values for reciprocating machines. (ISO 10816-6)

# Thermoelectric harvesters



## Strategy and device layouts

**Goal:** Obtain all-silicon thermoelectric micronanogenerators by means of the integration of silicon based NW arrays (as thermoelectric material) into a Si micromachined structure able to exploit a waste heat source to develop an internal thermal contrast between two isolated silicon parts.

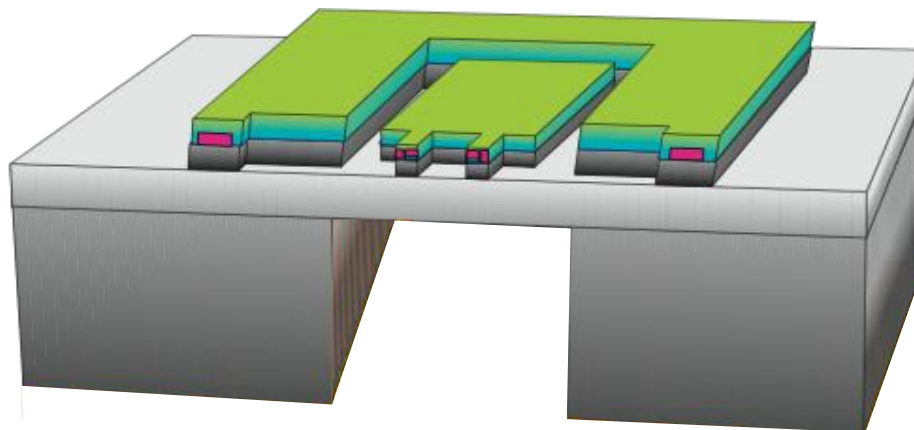


## Bottom-up strategy – Device layout

NWs will be grown with a VLS-CVD method that allows the in-situ integration of large density arrays of NWs within a 3D structure without specific nanolithography techniques.

## Process workflow

- Deposition of gold nanoparticles on device trenches by Galvanic Displacement
- ↓
- Growth of silicon nanowires on CVD by VLS synthesis
- ↓
- Removal of membrane and passivation oxide with HF
- ↓
- Drying of the device with nanowires by Critical Point Drying/Freeze Drying



Dávila et al, J. Elect. Mat., Vol. 40, No. 5, 2011

NMP3-SL-2013-604169

## Process workflow

① Deposition of gold nanoparticles on device trenches by Galvanic Displacement



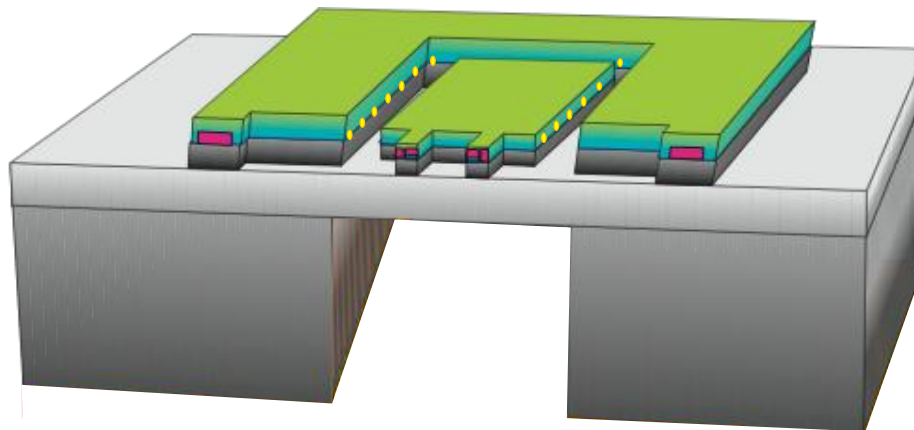
- Growth of silicon nanowires on CVD by VLS synthesis



- Removal of membrane and passivation oxide with HF



- Drying of the device with nanowires by Critical Point Drying/Freeze Drying

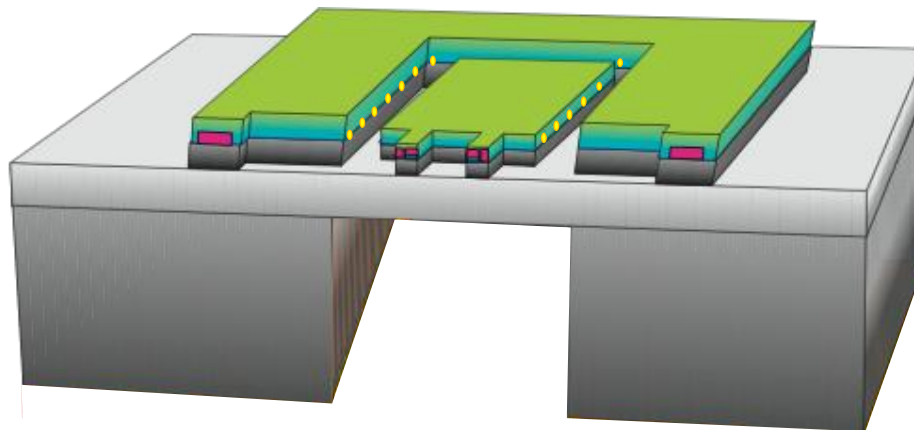


Dávila et al, J. Elect. Mat., Vol. 40, No. 5, 2011

NMP3-SL-2013-604169

## Process workflow

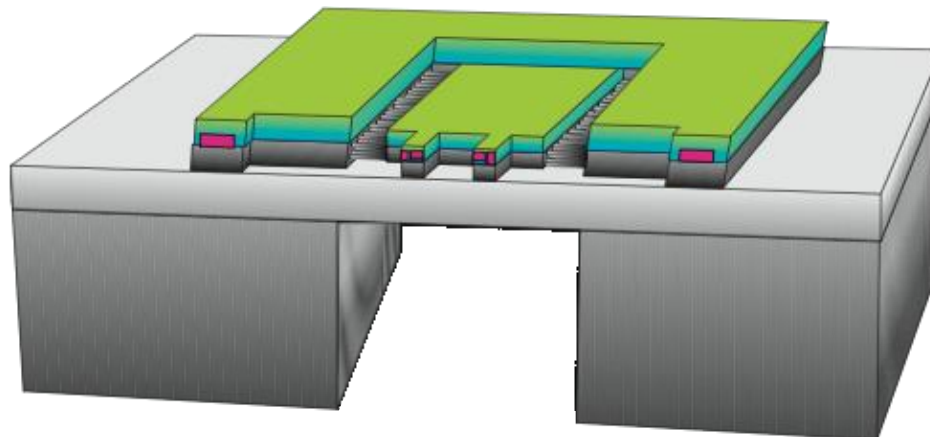
- ① Deposition of gold nanoparticles on device trenches by Galvanic Displacement
- ↓
- ② Growth of silicon nanowires on CVD by VLS synthesis
- ↓
- Removal of membrane and passivation oxide with HF
- ↓
- Drying of the device with nanowires by Critical Point Drying/Freeze Drying



Dávila et al, J. Elect. Mat., Vol. 40, No. 5, 2011

## Process workflow

- Deposition of gold nanoparticles on device trenches by Galvanic Displacement
- ⇓
- ⊙ Growth of silicon nanowires on CVD by VLS synthesis
- ⇓
- Removal of membrane and passivation oxide with HF
- ⇓
- Drying of the device with nanowires by Critical Point Drying/Freeze Drying

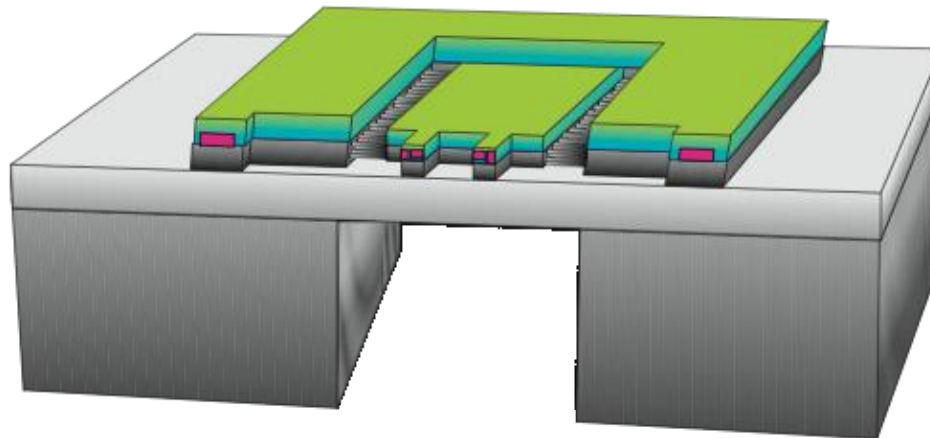


Dávila et al, J. Elect. Mat., Vol. 40, No. 5, 2011

NMP3-SL-2013-604169

## Process workflow

- Deposition of gold nanoparticles on device trenches by Galvanic Displacement
- ↓
- ⊙ Growth of silicon nanowires on CVD by VLS synthesis
- ↓
- ⊙ Removal of membrane and passivation oxide with HF
- ↓
- ⊙ Drying of the device with nanowires by Critical Point Drying/Freeze Drying

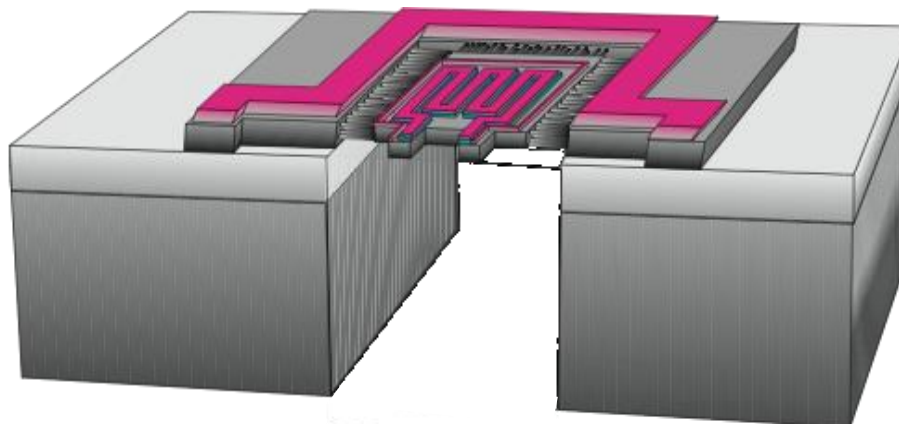


Dávila et al, J. Elect. Mat., Vol. 40, No. 5, 2011

NMP3-SL-2013-604169

## Process workflow

- Deposition of gold nanoparticles on device trenches by Galvanic Displacement
- ↓
- Growth of silicon nanowires on CVD by VLS synthesis
- ↓
- ⊙ Removal of membrane and passivation oxide with HF
- ↓
- ⊙ Drying of the device with nanowires by Critical Point Drying/Freeze Drying



Dávila et al, J. Elect. Mat., Vol. 40, No. 5, 2011

NMP3-SL-2013-604169

## Microemulsion Galvanic Displacement

1 – Several microemulsions with different R values are prepared.

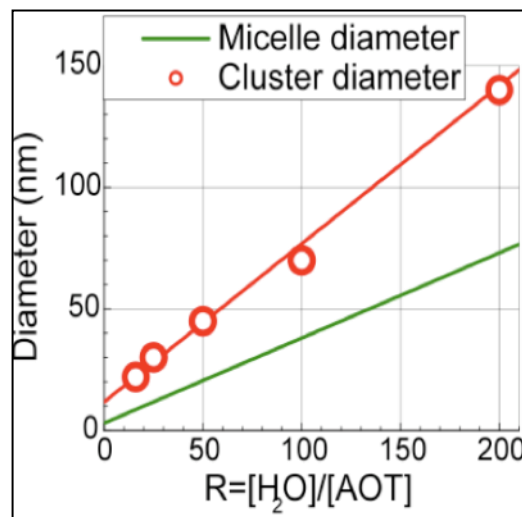
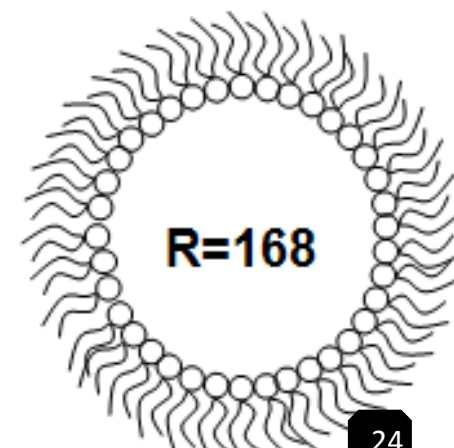
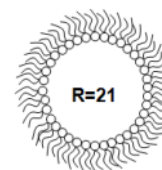
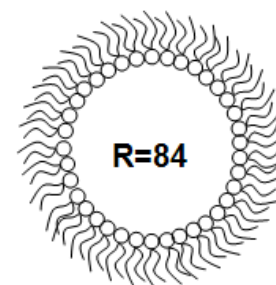
Aqueous phase: 0.2M HF + 0.01M  $\text{KAuCl}_4$

+

Organic phase: 0.33M AOT (surfactant) in n-heptane



$$R = \frac{[\text{Water}]}{[\text{Surfactant}]} = \frac{[\text{H}_2\text{O}]}{[\text{AOT}]}$$



NMP3-SL-2013-604169

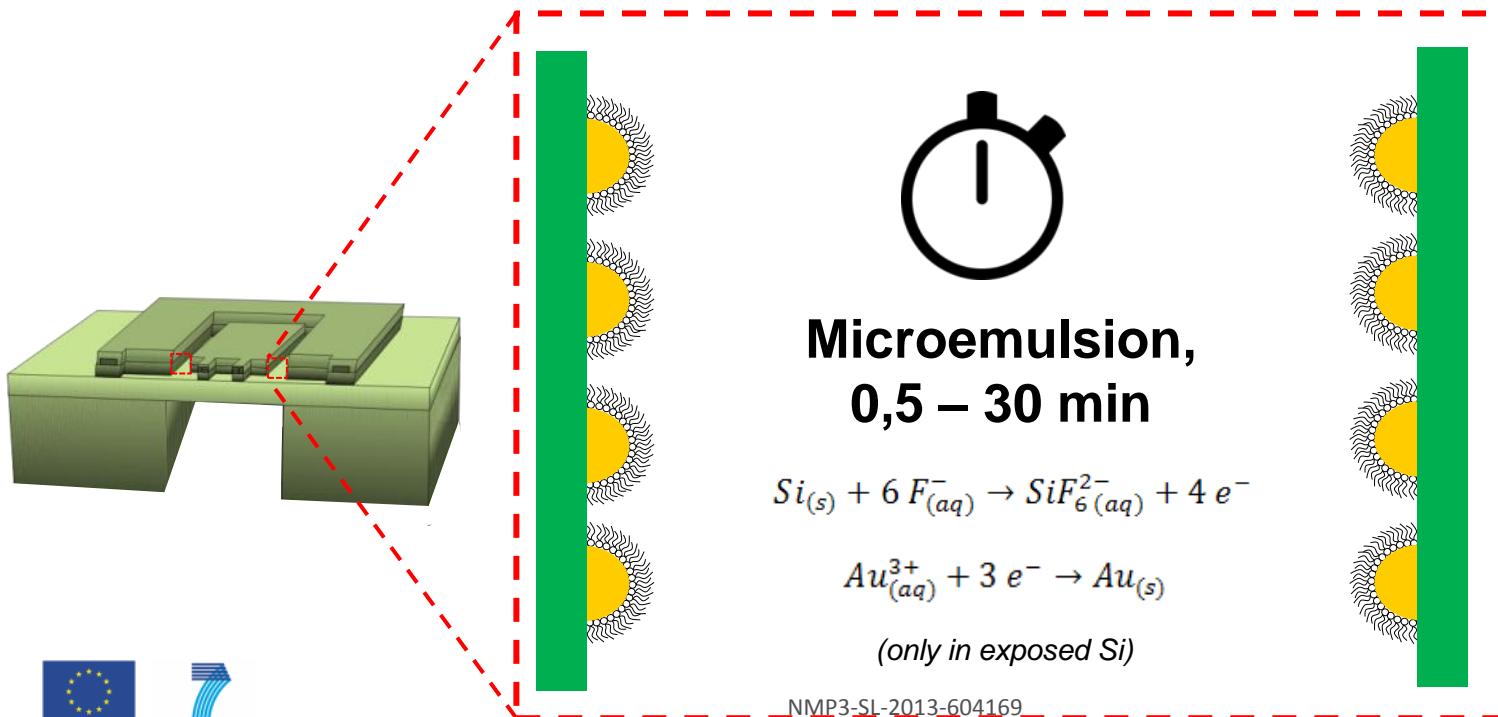


## Microemulsion Galvanic Displacement

- 1 – Several **microemulsions** with different R values are **prepared**.
- 2 – Devices are **dipped in HF** in order to remove native oxide from trenches

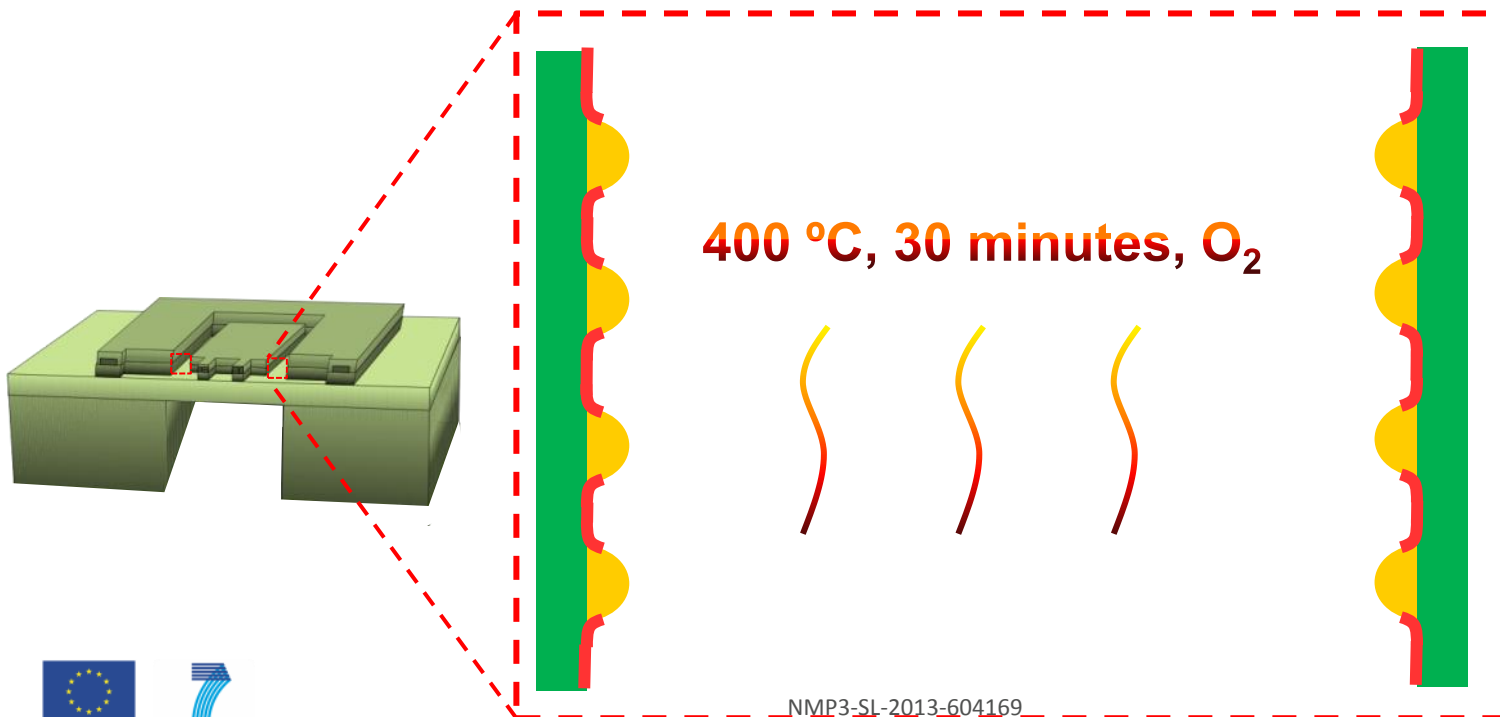
## Microemulsion Galvanic Displacement

- 1 – Several **microemulsions** with different R values are **prepared**.
- 2 – Devices are **dipped in HF** in order to remove native oxide from trenches
- 3 – Devices are **dipped in microemulsions** during a controlled dipping time. Gold NPs are formed



## Microemulsion Galvanic Displacement

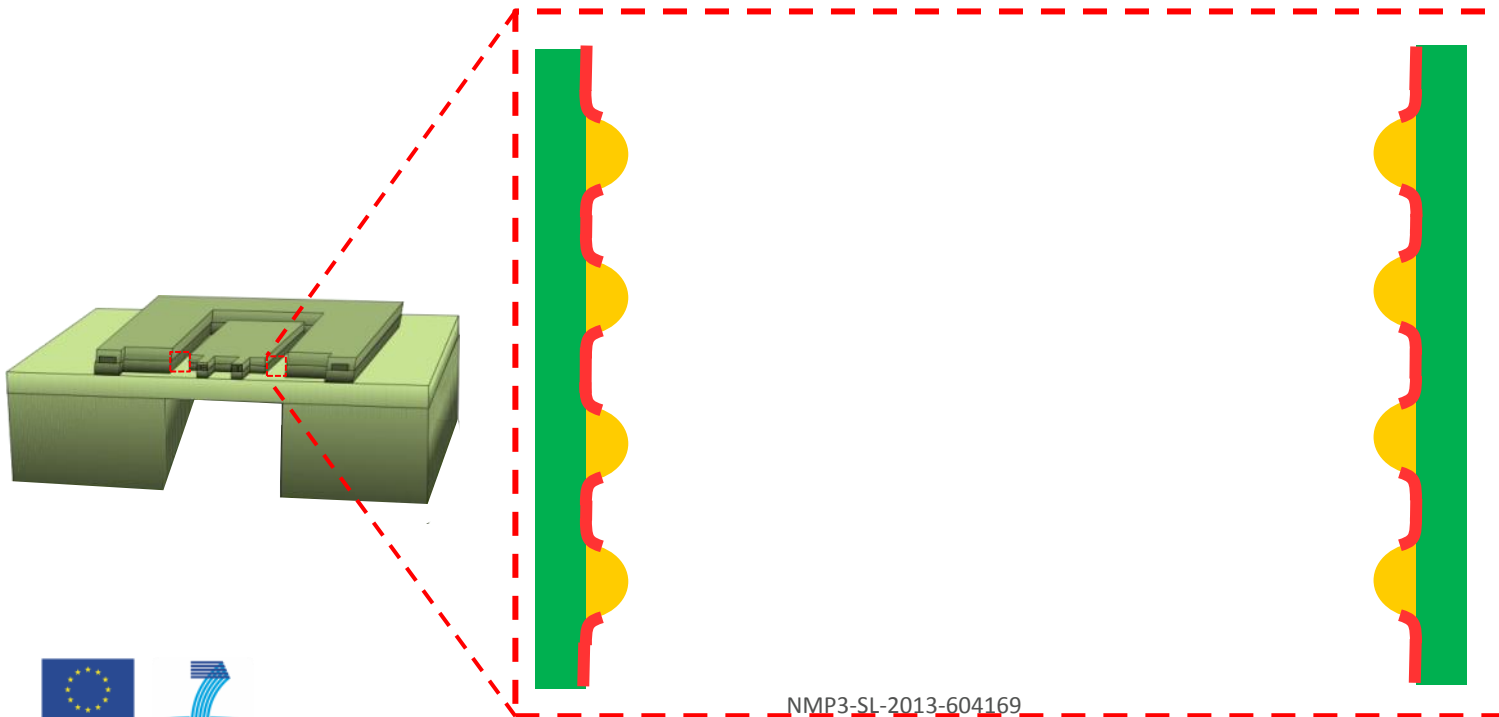
- 1 – Several **microemulsions** with different R values are **prepared**.
- 2 – Devices are **dipped in HF** in order to remove native oxide from trenches
- 3 – Devices are **dipped in microemulsions** during a controlled dipping time. Gold NPs are formed
- 4 – Devices are **annealed** to remove the remaining surfactant



NMP3-SI-2013-604169

## Microemulsion Galvanic Displacement

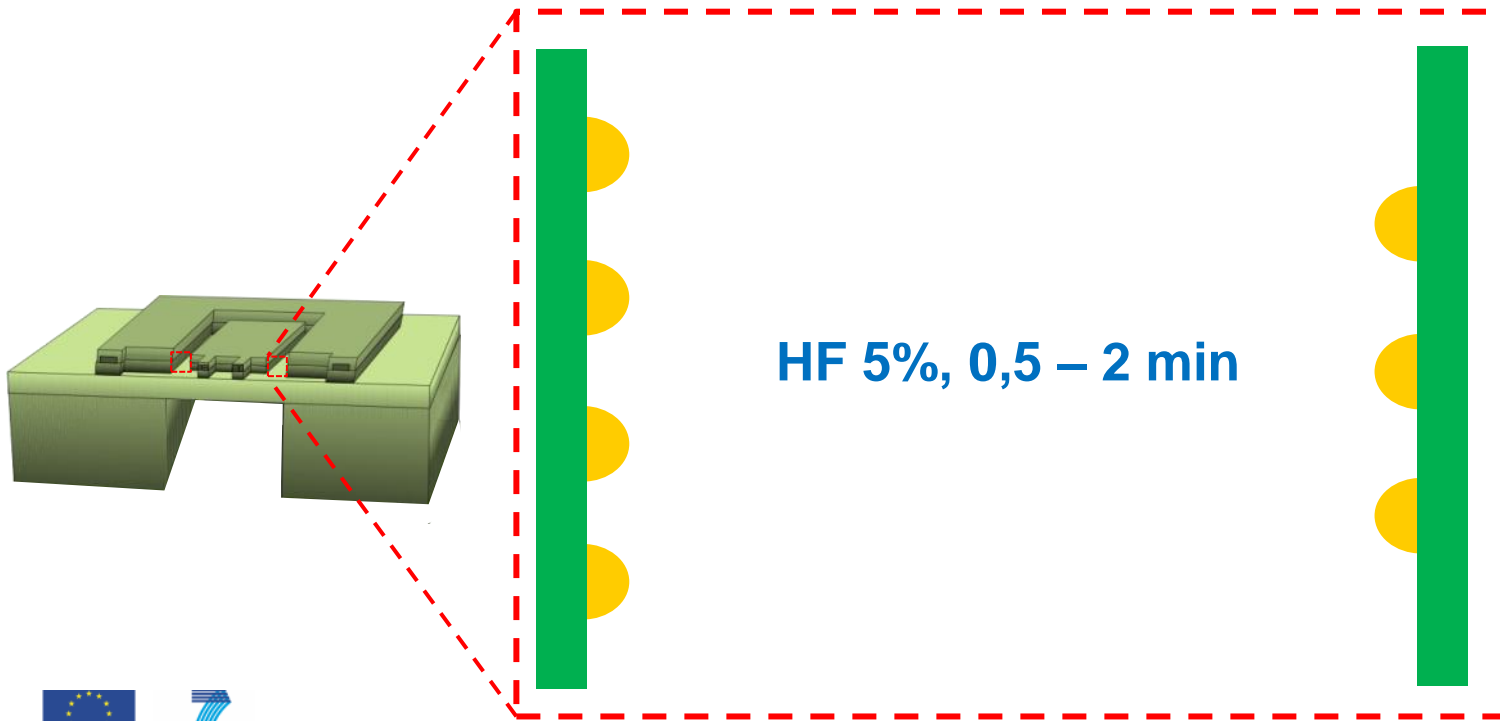
- 1 – Several **microemulsions** with different R values are **prepared**.
- 2 – Devices are **dipped in HF** in order to remove native oxide from trenches
- 3 – Devices are **dipped in microemulsions** during a controlled dipping time. Gold NPs are formed
- 4 – Devices are **annealed** to remove the remaining surfactant



NMP3-SI-2013-604169

## CVD-VLS growth of silicon nanowires

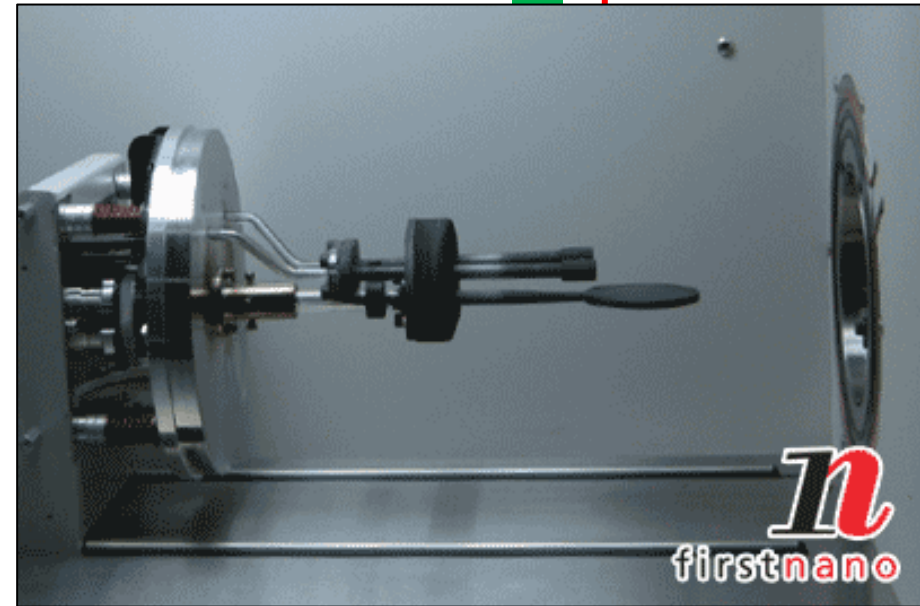
1 – Devices are dipped in **HF** in order to remove thermal oxide formed during calcination



NMP3-SL-2013-604169

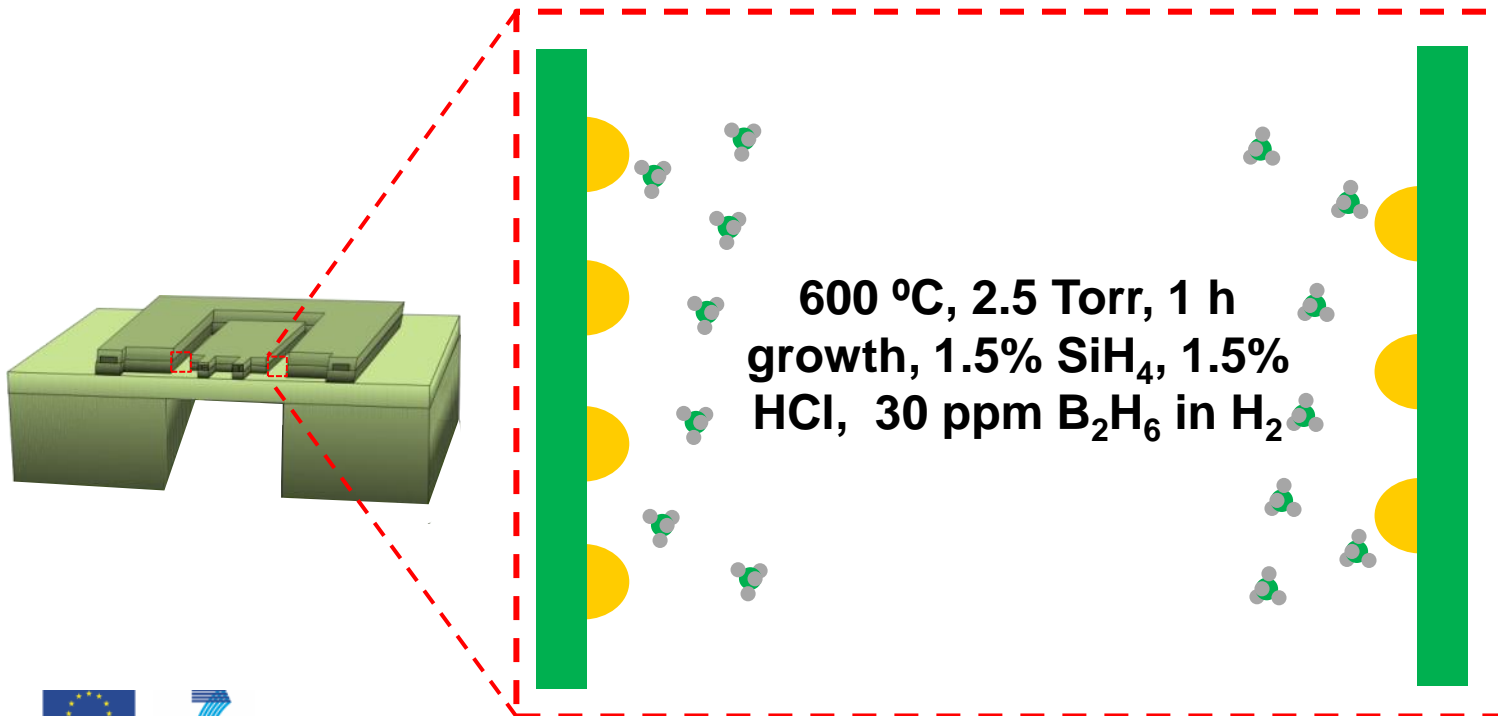
## CVD-VLS growth of silicon nanowires

- 1 – Devices are dipped in **HF** in order to remove thermal oxide formed during calcination
- 2 – Devices are loaded into **CVD**



## CVD-VLS growth of silicon nanowires

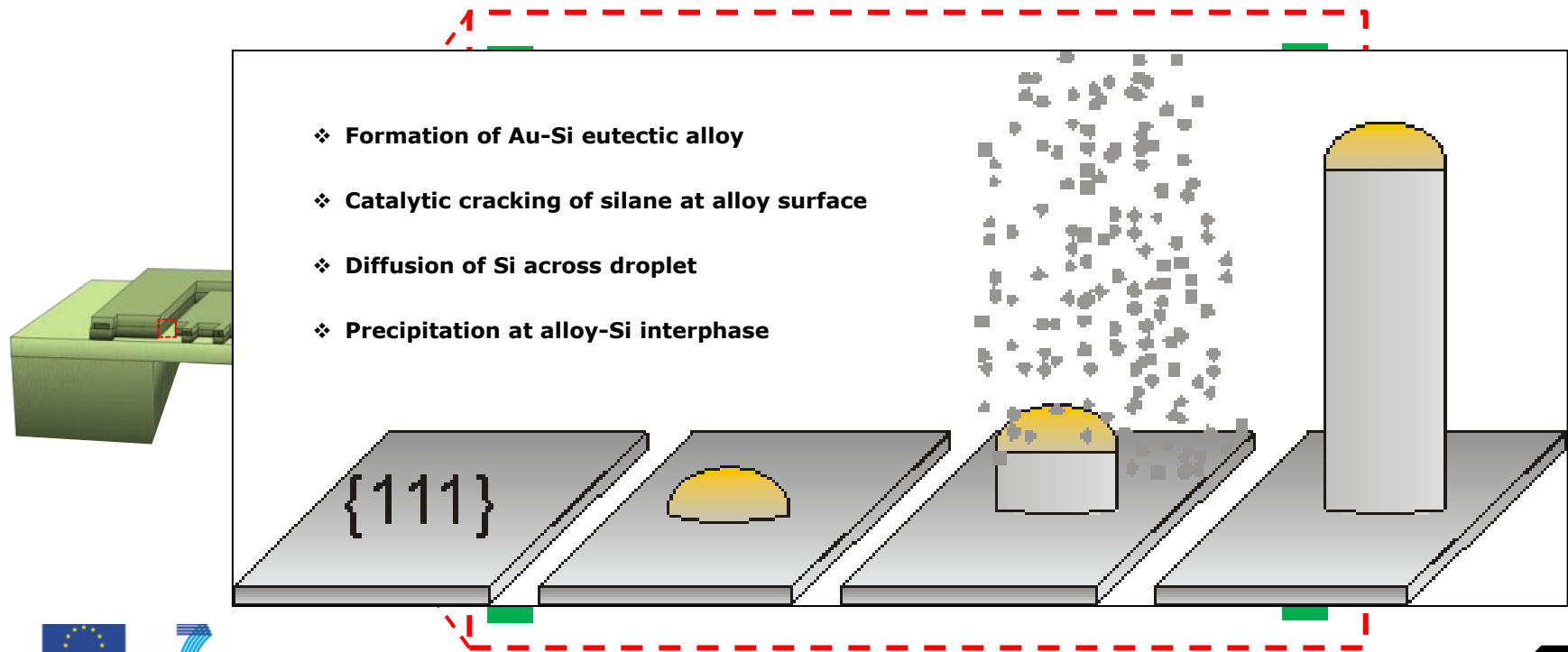
- 1 – Devices are dipped in **HF** in order to remove thermal oxide formed during calcination
- 2 – Devices are loaded into **CVD**
- 3 – These devices are brought to **reaction conditions and exposed to silane**. Silicon nanowires are grown by VLS synthesis



NMP3-SL-2013-604169

## CVD-VLS growth of silicon nanowires

- 1 – Devices are dipped in **HF** in order to remove thermal oxide formed during calcination
- 2 – Devices are loaded into **CVD**
- 3 – These devices are brought to **reaction conditions and exposed to silane**. Silicon nanowires are grown by VLS synthesis

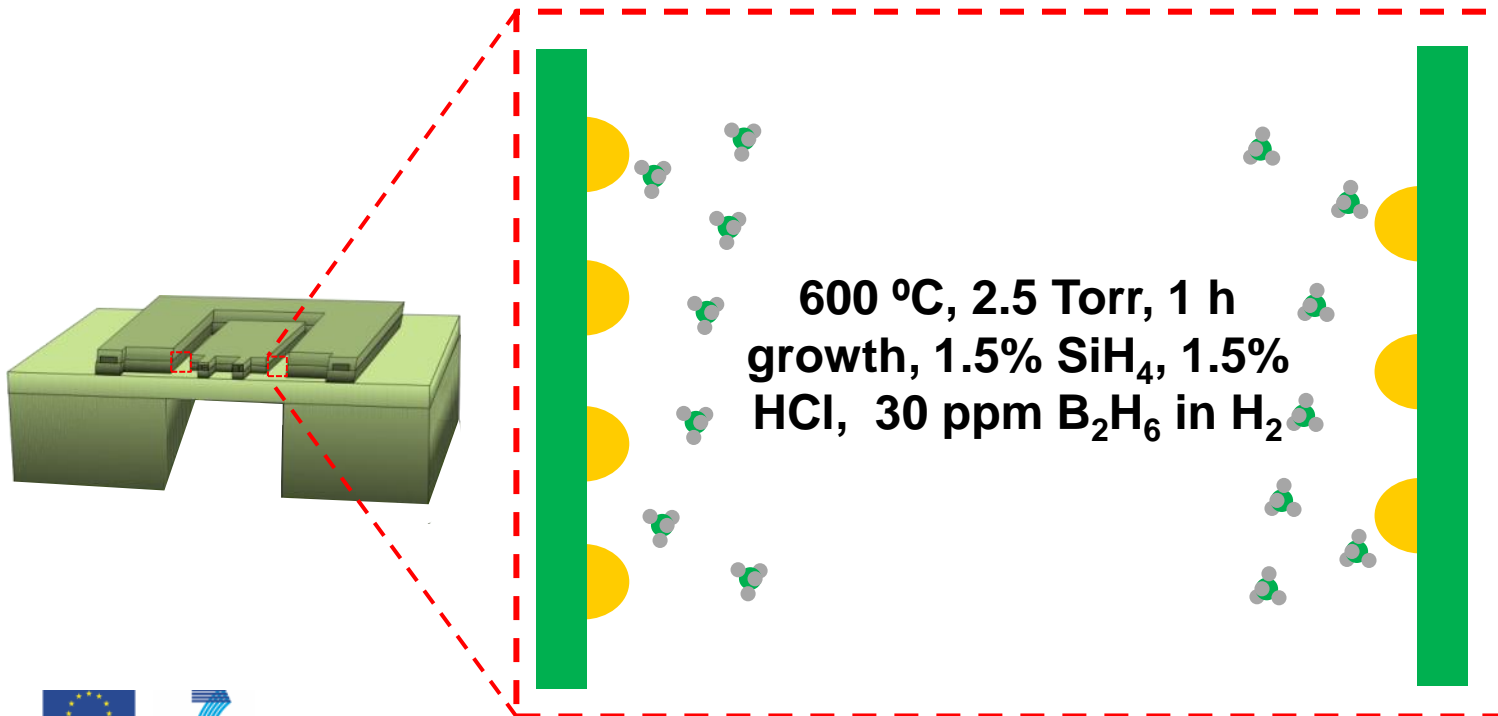


NMP3-SL-2013-604169



## CVD-VLS growth of silicon nanowires

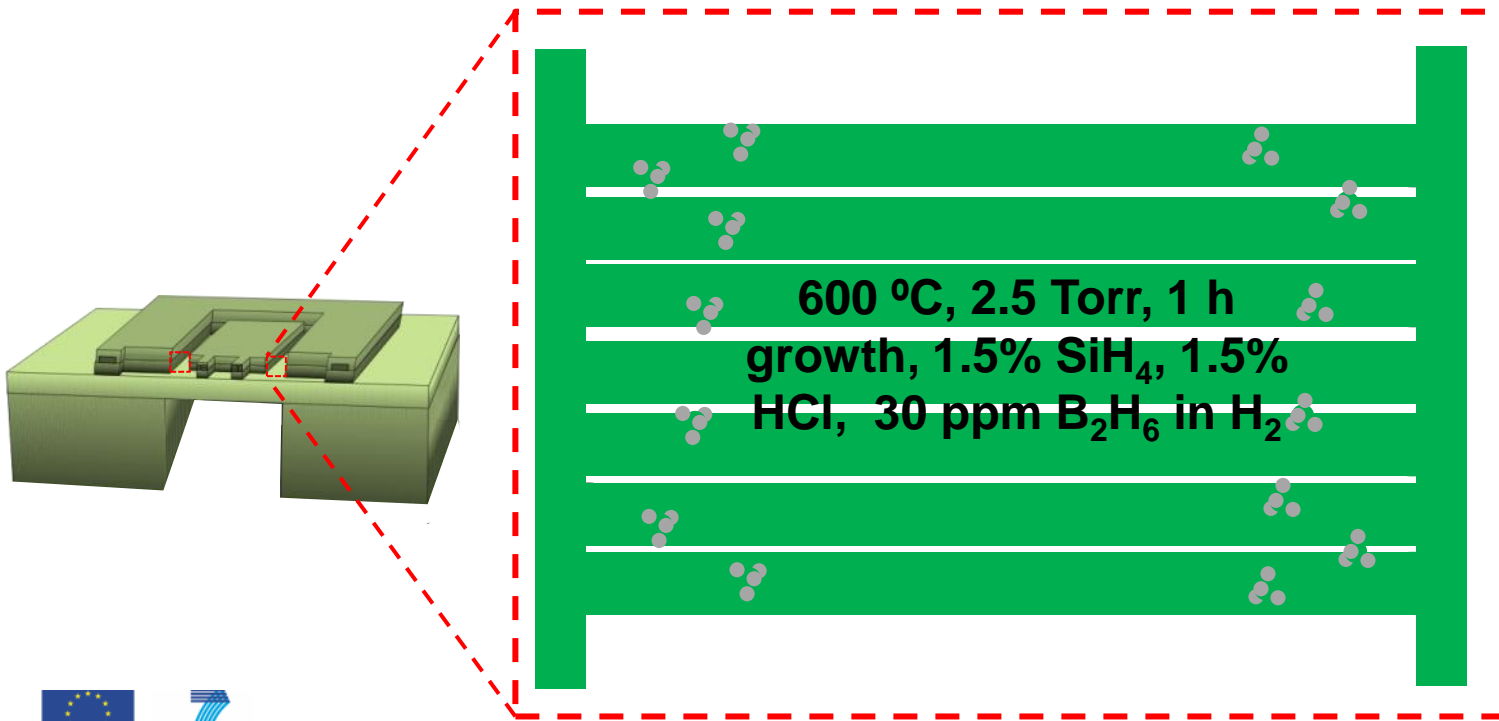
- 1 – Devices are dipped in **HF** in order to remove thermal oxide formed during calcination
- 2 – Devices are loaded into **CVD**
- 3 – These devices are brought to **reaction conditions and exposed to silane**. Silicon nanowires are grown by VLS synthesis



NMP3-SL-2013-604169

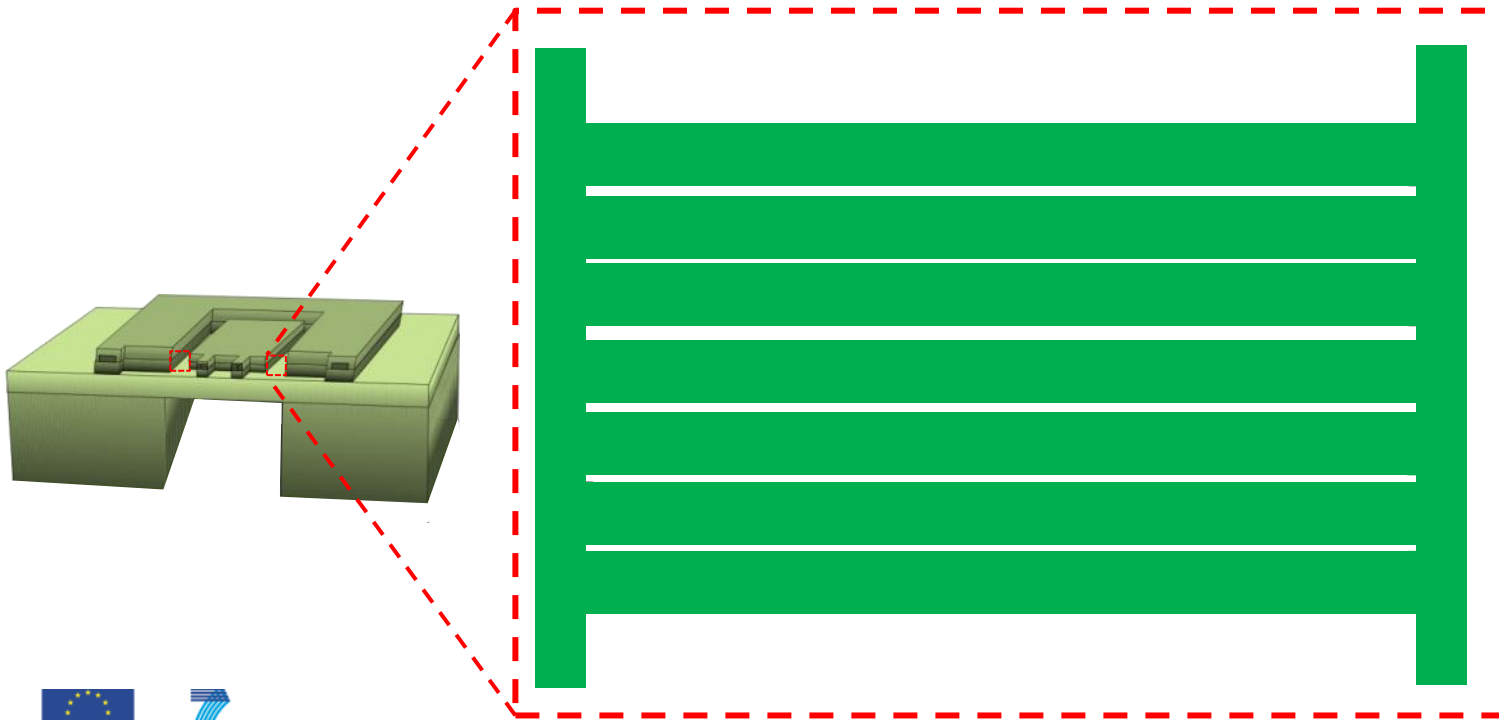
## CVD-VLS growth of silicon nanowires

- 1 – Devices are dipped in **HF** in order to remove thermal oxide formed during calcination
- 2 – Devices are loaded into **CVD**
- 3 – There devices are brought to **reaction conditions and exposed to silane**. Silicon nanowires are grown by VLS synthesis



## CVD-VLS growth of silicon nanowires

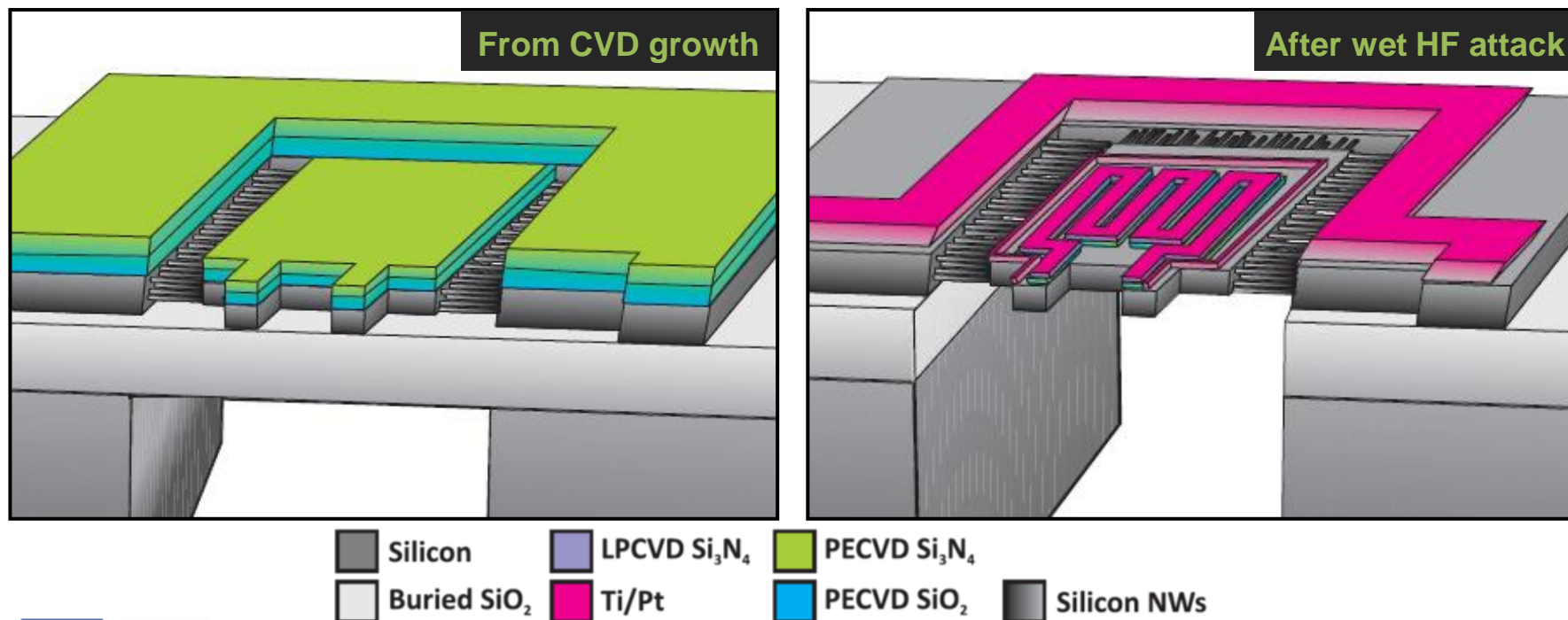
- 1 – Devices are dipped in **HF** in order to remove thermal oxide formed during calcination
- 2 – Devices are loaded into **CVD**
- 3 – There devices are brought to **reaction conditions and exposed to silane**. Silicon nanowires are grown by VLS synthesis



NMP3-SL-2013-604169

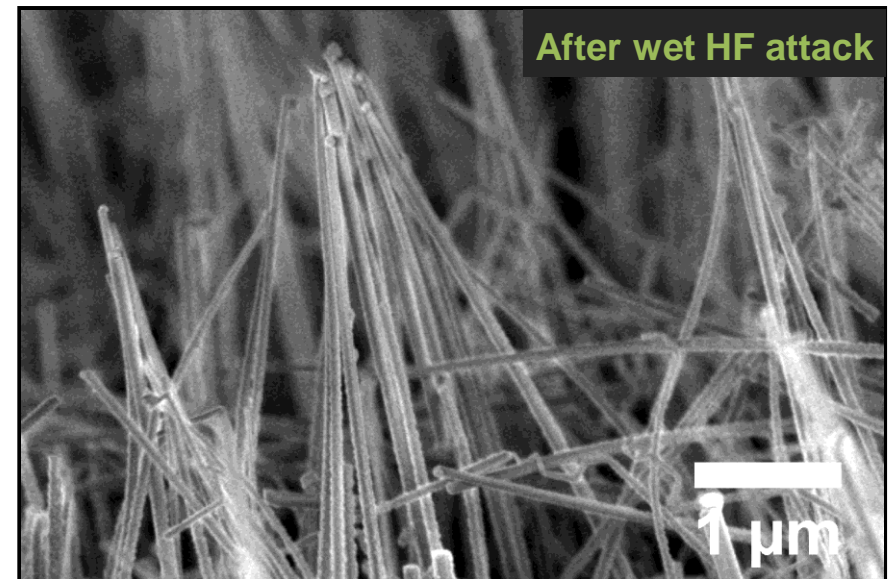
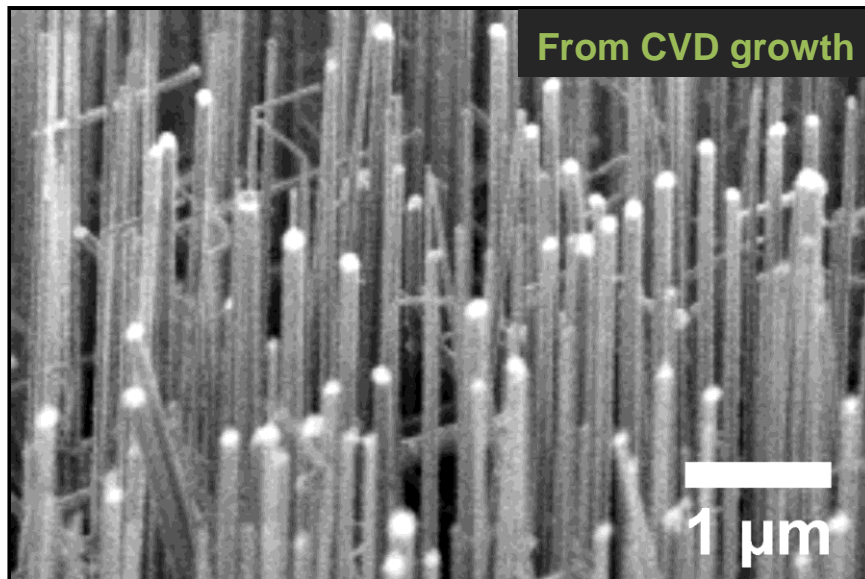
## Membrane removal in HF

After growing Si NWs in a  $\mu$ TEG device a wet attack in HF must be performed in order to remove membrane and passivation silicon oxide – which covers contacts.



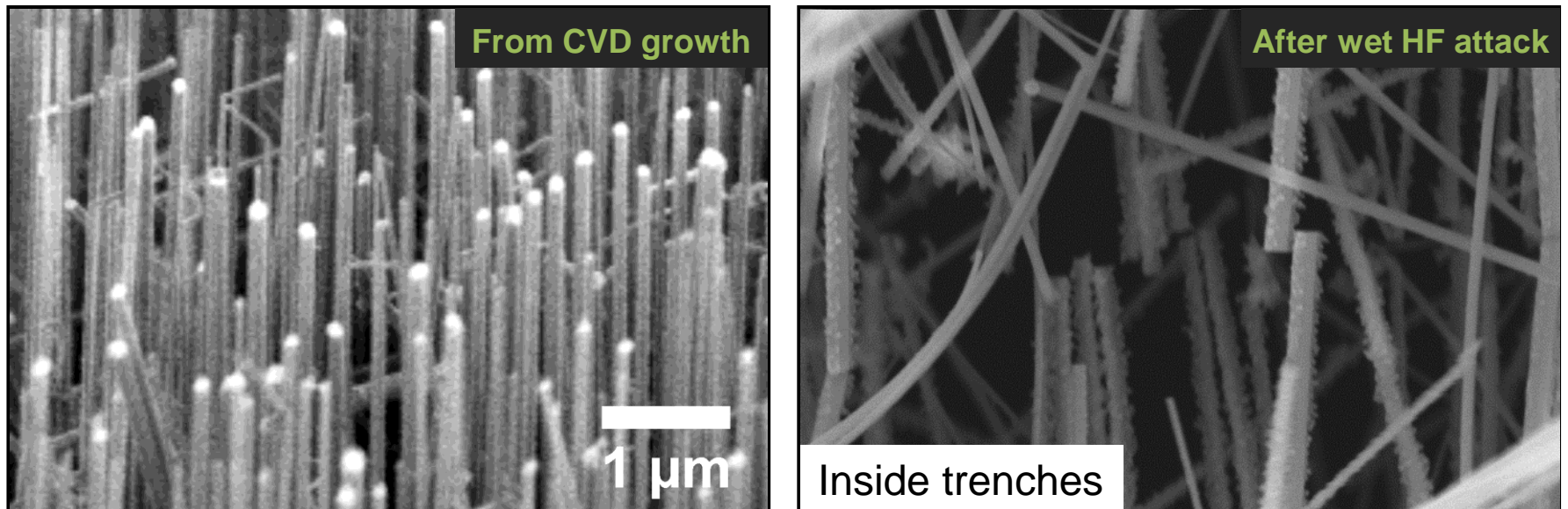
## Membrane removal in HF

After growing Si NWs in a  $\mu$ TEG device a wet attack in HF must be performed in order to remove membrane and passivation silicon oxide – which covers contacts.

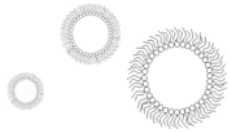


## Membrane removal in HF

After growing Si NWs in a  $\mu$ TEG device a wet attack in HF must be performed in order to remove membrane and passivation silicon oxide – which covers contacts.

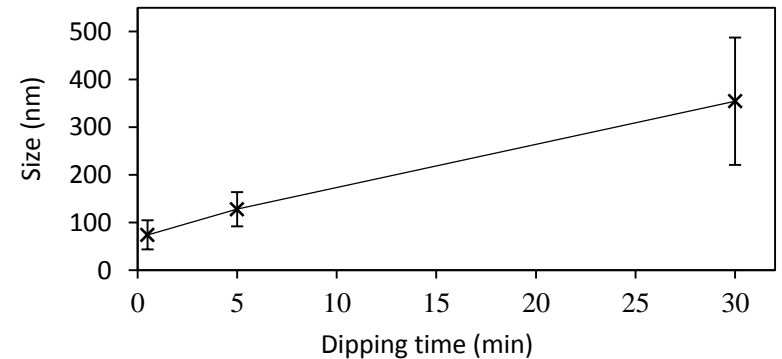
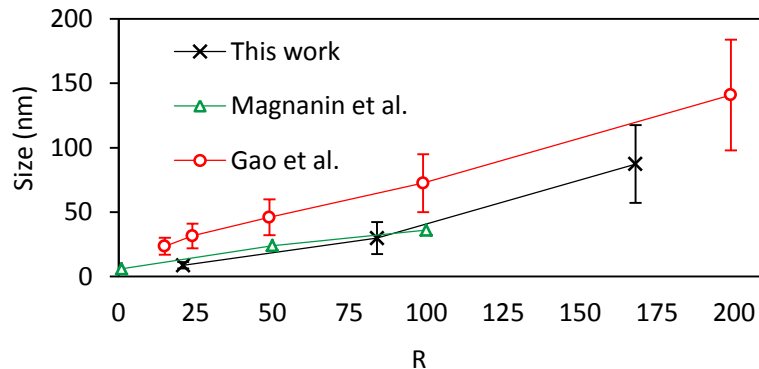
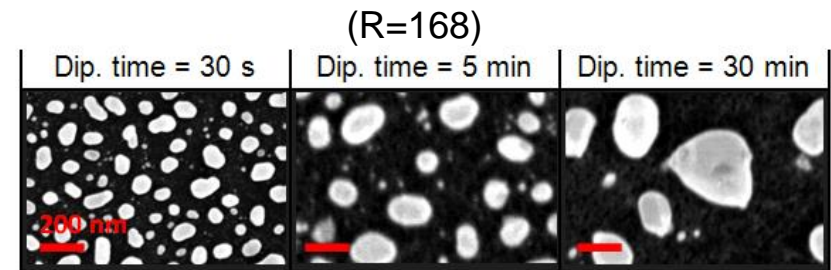
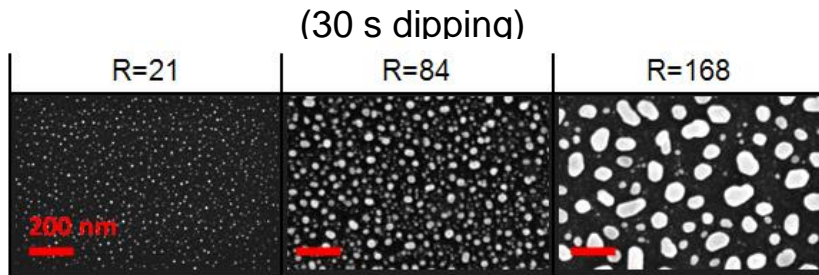


## Galvanic Displacement – Catalyst control



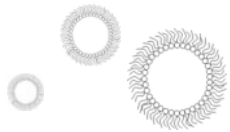
- Effects of R of the microemulsion

- Effects of dipping time in the microemulsion



❖ Au NPs size increases with R and dipping time

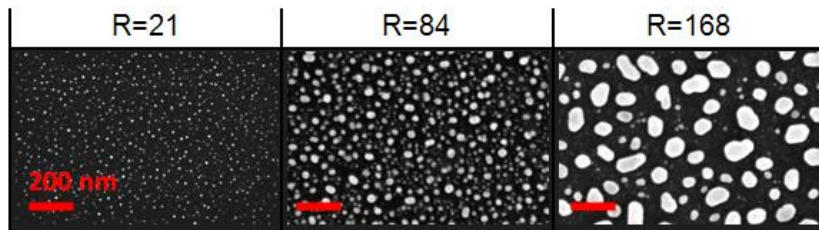
## Galvanic Displacement – Catalyst control



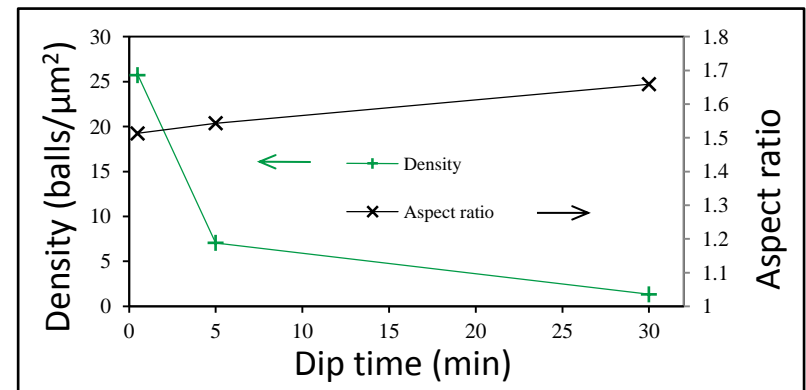
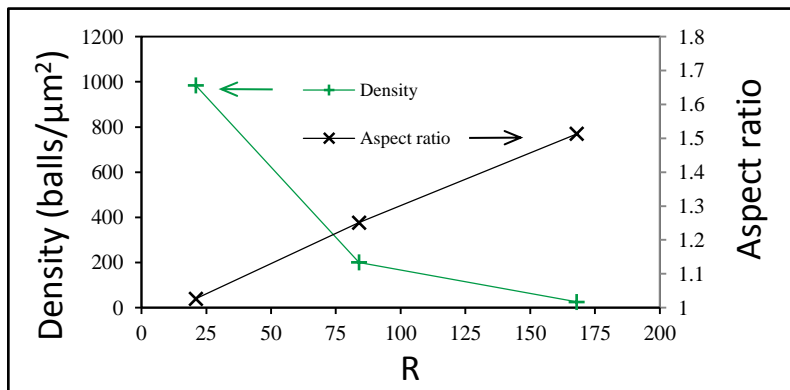
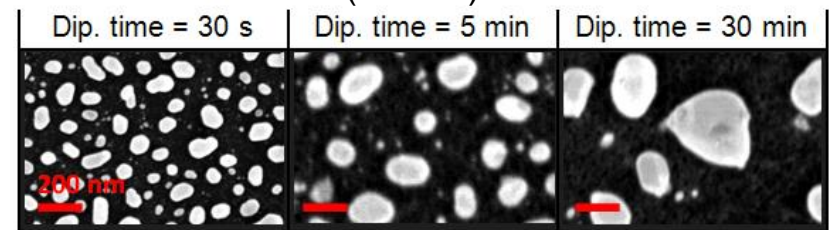
- Effects of R of the microemulsion

- Effects of dipping time in the microemulsion

(30 s dipping)



(R=168)



❖ Au NPs size increases with R and dipping time

❖ Density decreases with R and dipping time

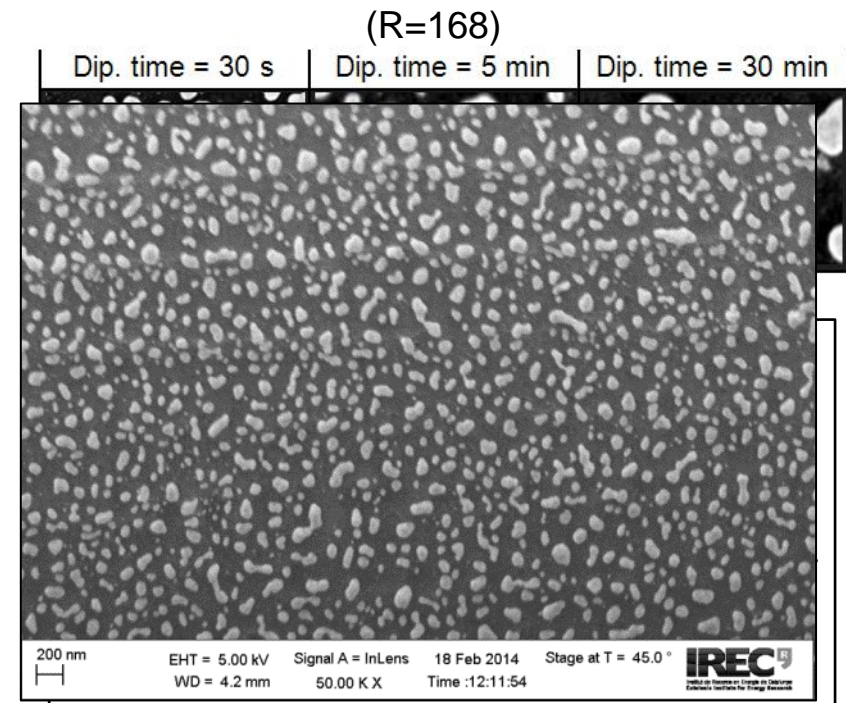
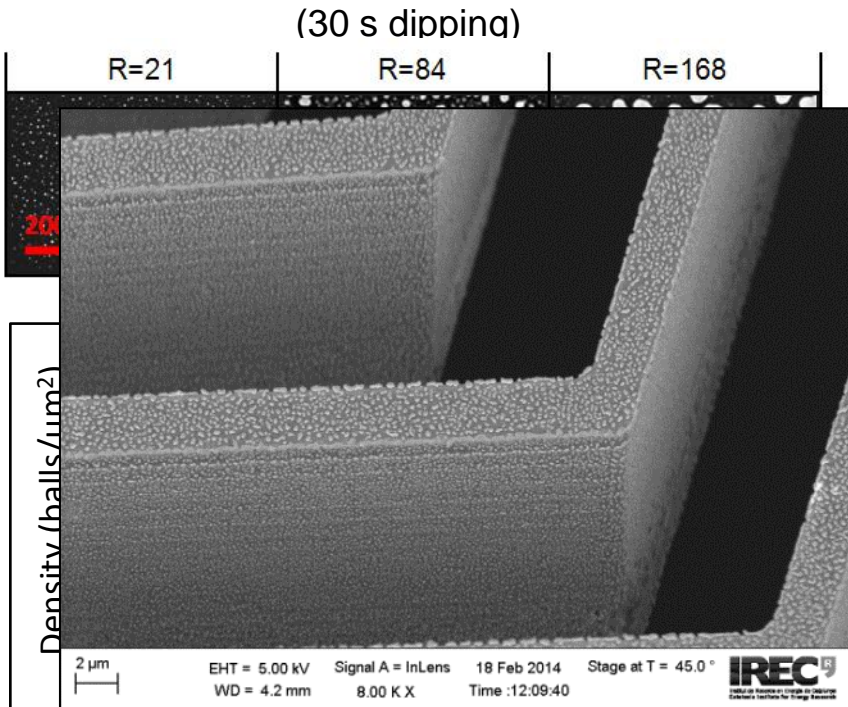


## Galvanic Displacement – Catalyst control



- Effects of R of the microemulsion

- Effects of dipping time in the microemulsion

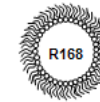
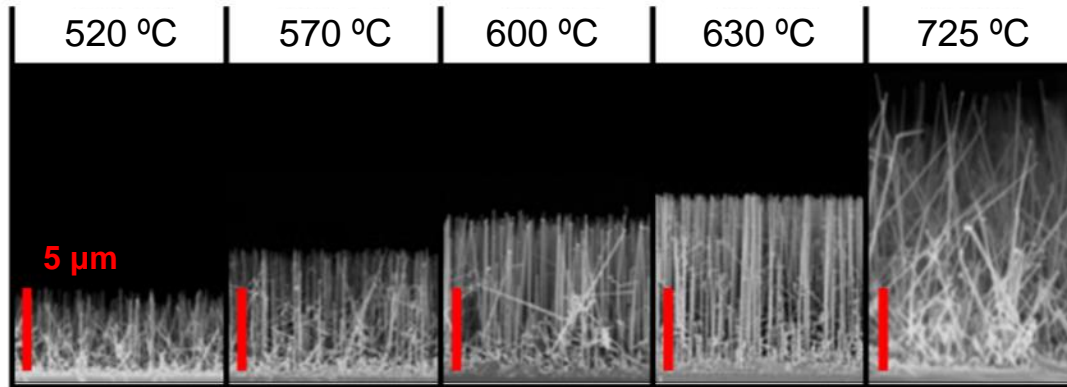


❖ Au NPs size increases with R and dipping time

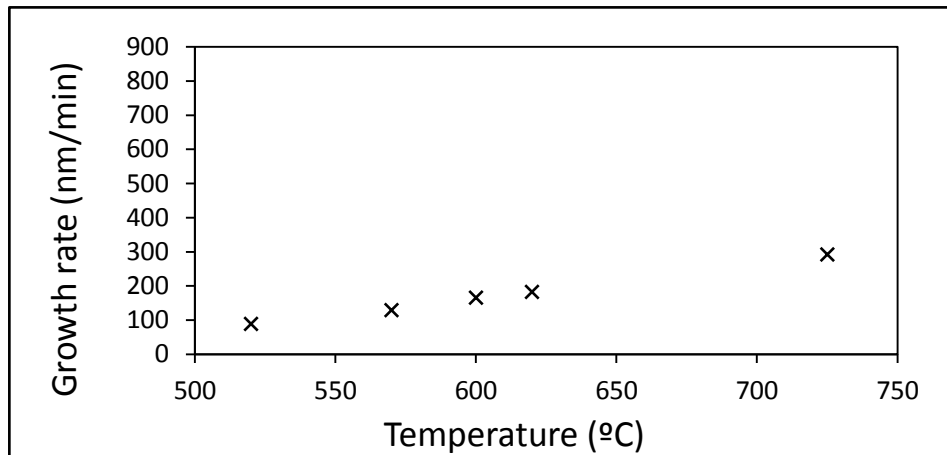
❖ Density decreases with R and dipping time

NMP3-SL-2013-604169

## CVD-VLS – Nanowire control – Effect of temperature



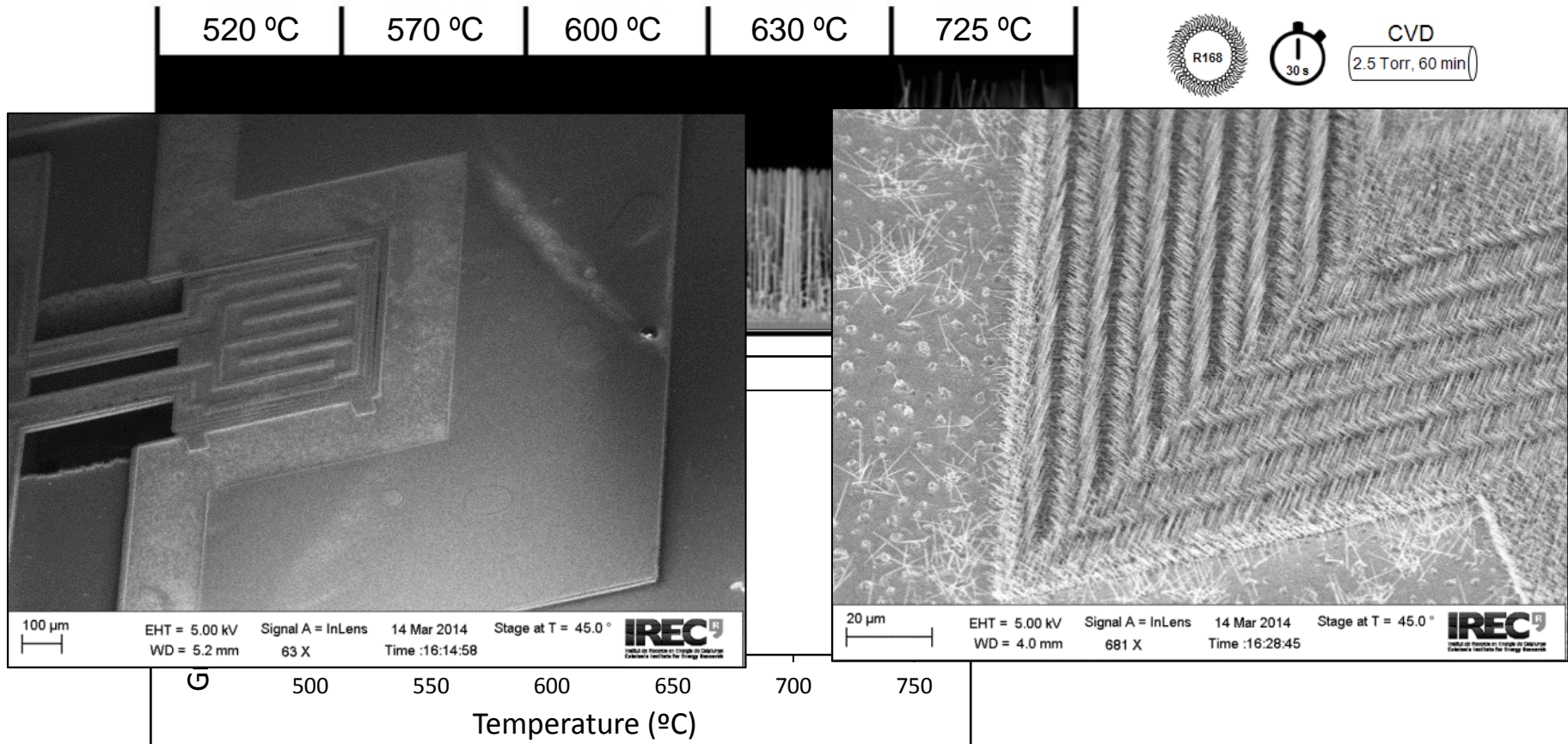
CVD  
2.5 Torr, 60 min



❖ Growth rate increases with T

❖ Verticality has a maximum in 630 °C

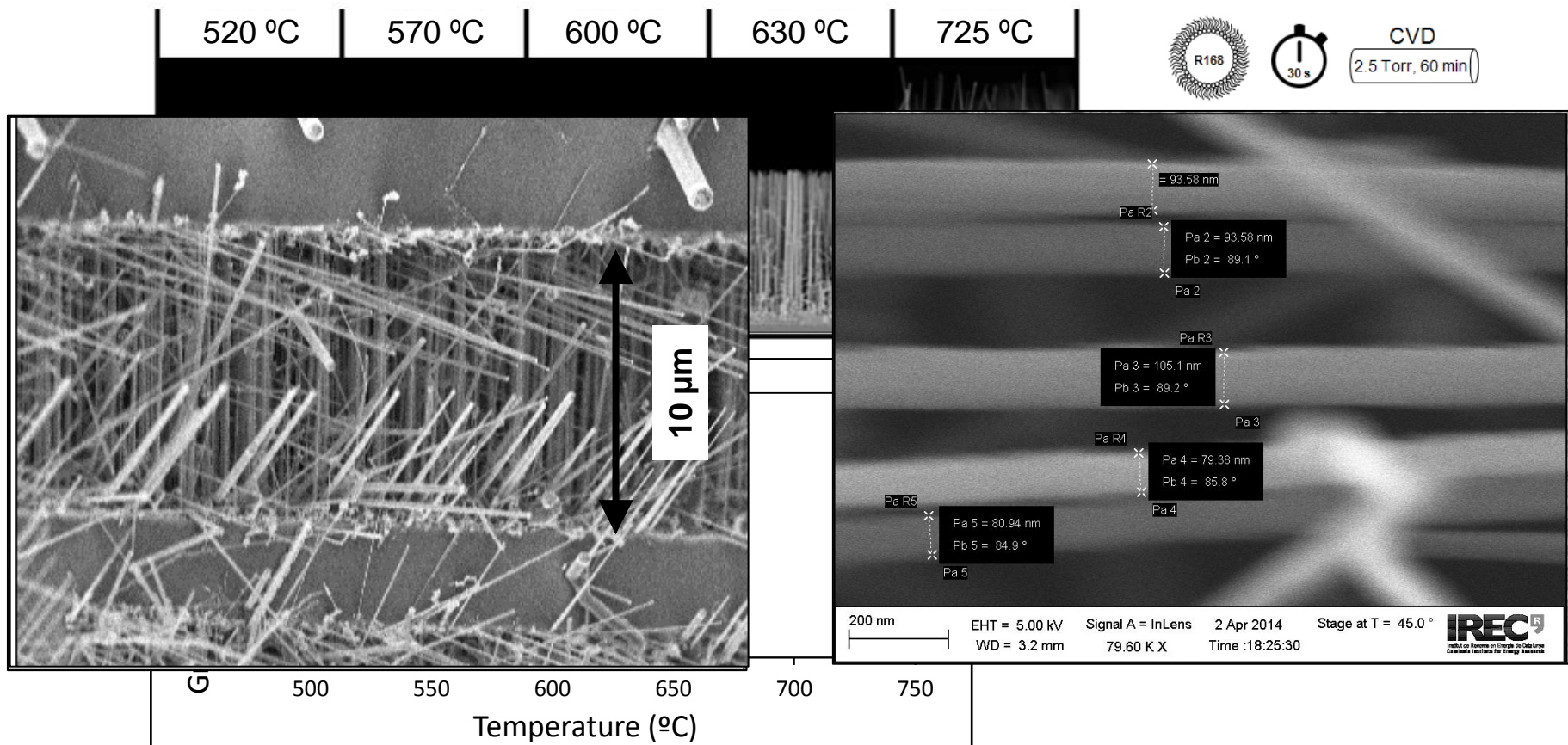
## CVD-VLS – Nanowire control – Effect of temperature



❖ Well aligned horizontal Si NWs were obtained in trenches

NMP3-SL-2013-604169

## CVD-VLS – Nanowire control – Effect of temperature



❖ Well aligned horizontal Si NWs were obtained in trenches

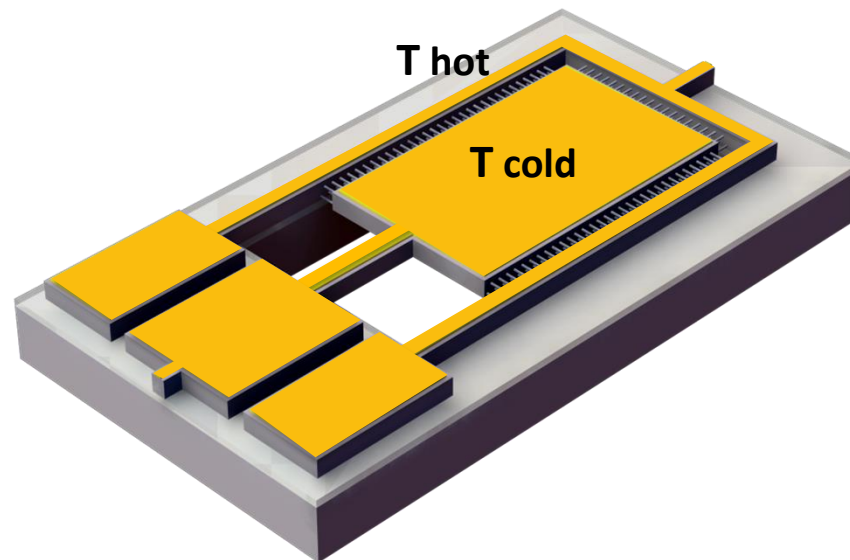
NMP3-SL-2013-604169

## Bottom-up strategy – Device layout

Structural core will be a Si device micromachined in such a way that hot and cold areas develop when resting on a hot surface.

**Hot area:** surrounding rim **Cold area:** suspended platform.

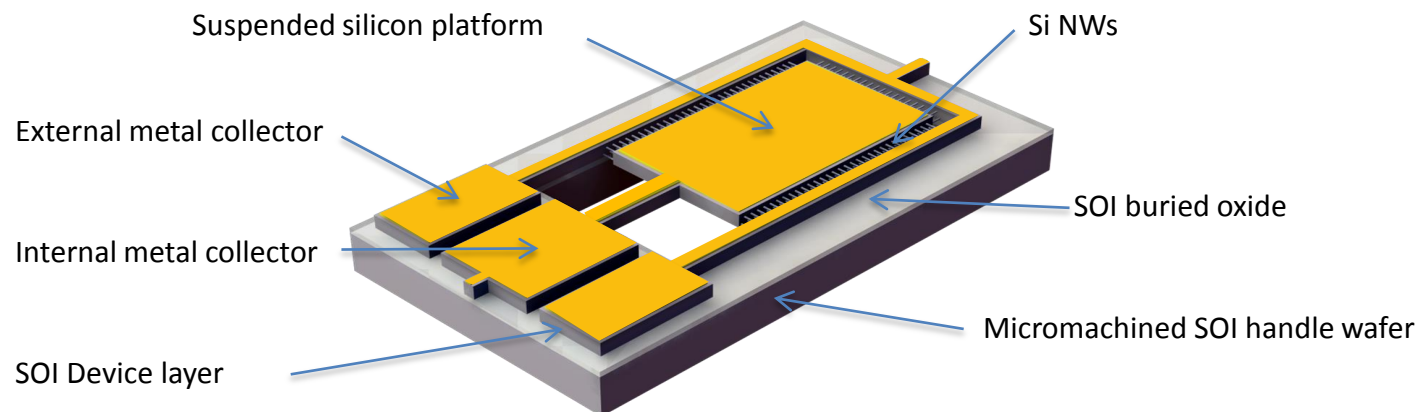
**Thermocouple:** nanostructured silicon and thin metal film.



NMP3-SL-2013-604169

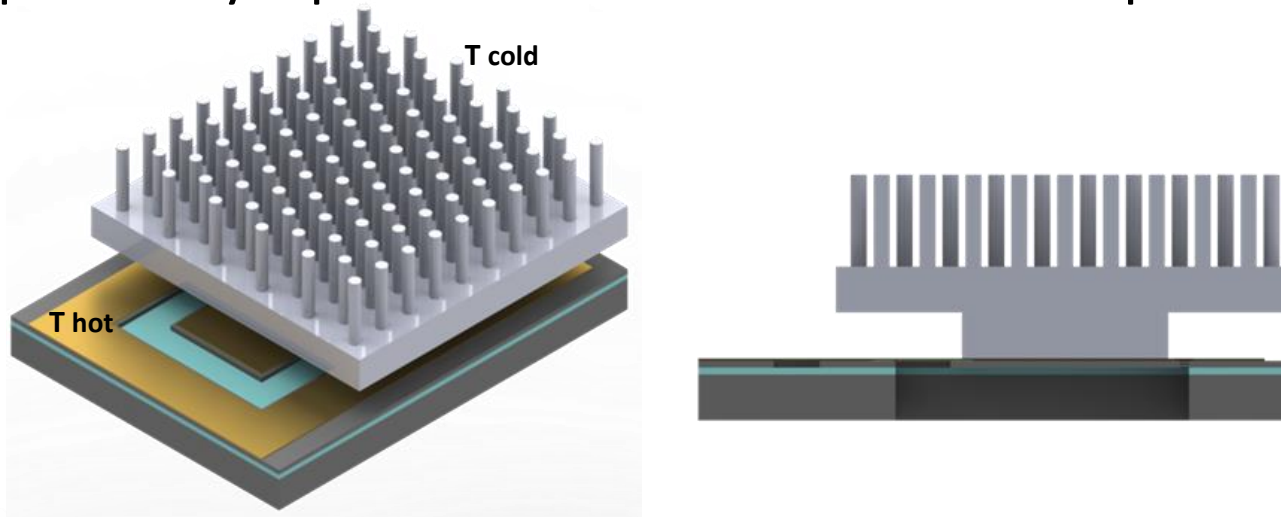
## Bottom-up strategy – Device layout

- SOI wafers used as starting material. Device layer  $\langle 110 \rangle$ , so that parallelograms with  $\langle 111 \rangle$  oriented walls can be built .
- Typical dimension will be 1 mm, with  $10 \mu\text{m}$  trench widths. Depth is fixed by device layer thickness, which will be around  $10\text{-}15 \mu\text{m}$  to accommodate a large number of NWs.



## Bottom-up strategy – Microradiator

- Integration of a microradiator in the cold side to efficiently convey into the active area the vertical thermal gradient present in the application scenario.
- Overhanging thermal conductive structure (metal/silicon) supported by a pillar in close contact with cold platform.



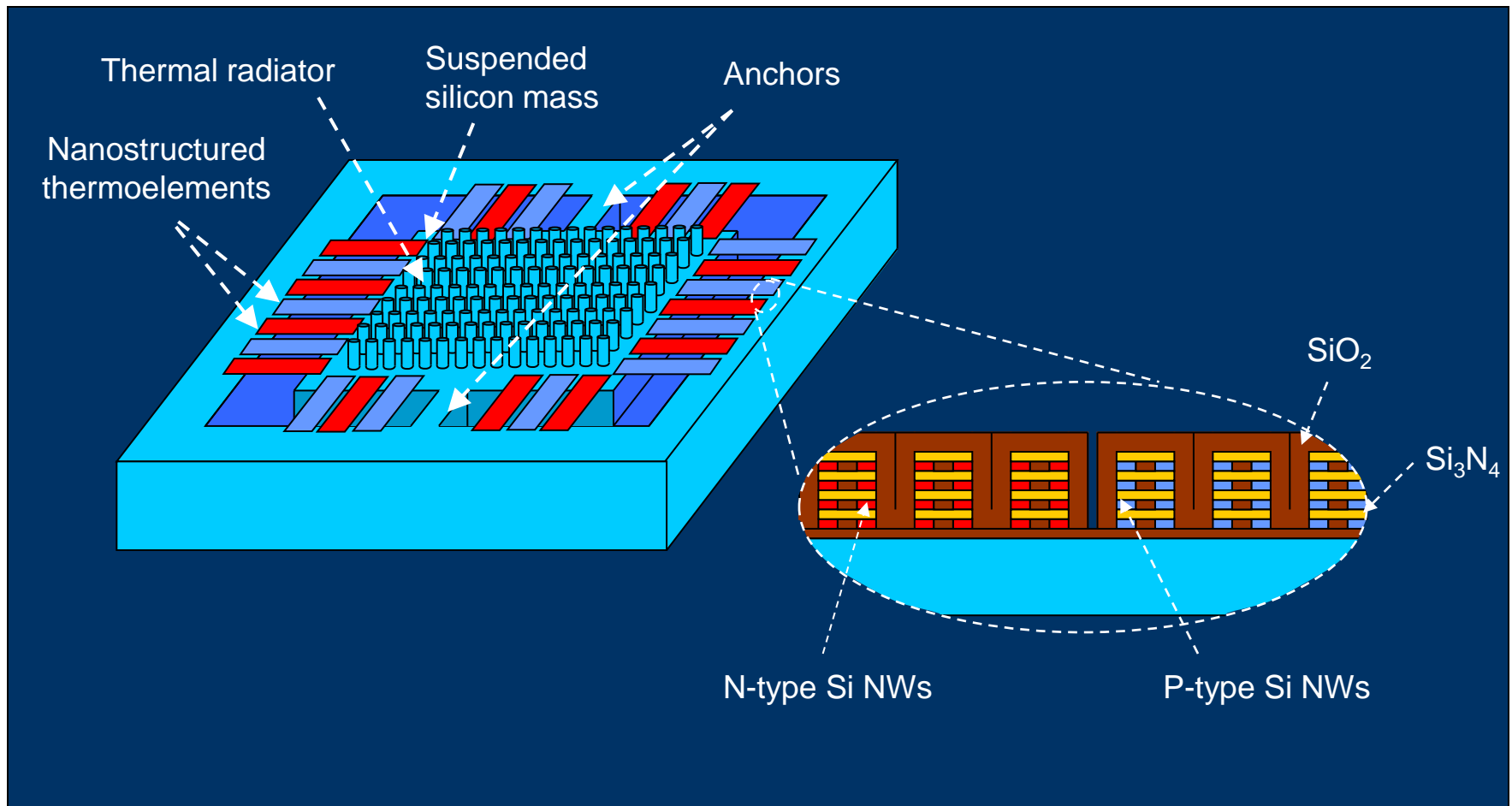
## Top-down strategy – Device layout

NWs will be grown with a CVD method within nanometric cavities built up by controlled etching and filling of recessed regions (without nanolithographic steps).

Semicond. Sci. Technol. 26 (2011) 045005



## Top-down layout with lateral NWs:



## Top-down fabrication of lateral NWs:

1. Si substrate



2. SiO<sub>2</sub> growth



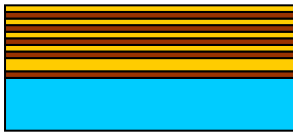
3. Si<sub>3</sub>N<sub>4</sub> deposition



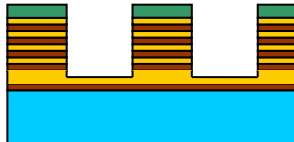
4. SiO<sub>2</sub> deposition



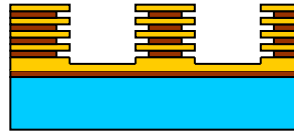
5. Si<sub>3</sub>N<sub>4</sub>/SiO<sub>2</sub> deposition



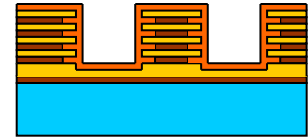
6. Si<sub>3</sub>N<sub>4</sub>/SiO<sub>2</sub> RIE



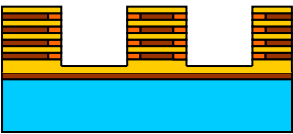
7. SiO<sub>2</sub> wet etching



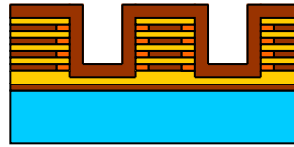
8. Poly deposition



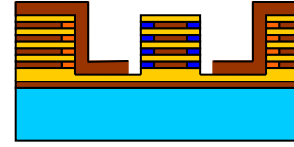
9. Poly etchback



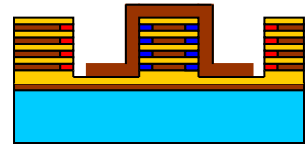
10. SiO<sub>2</sub> deposition



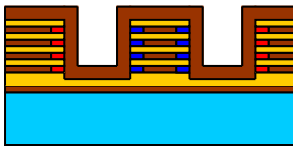
11. P-type doping



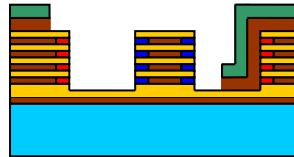
12. N-type doping



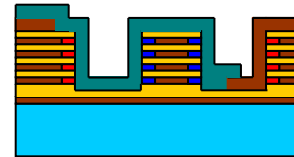
13. SiO<sub>2</sub> deposition



14. SiO<sub>2</sub> etching



15. Al patterning



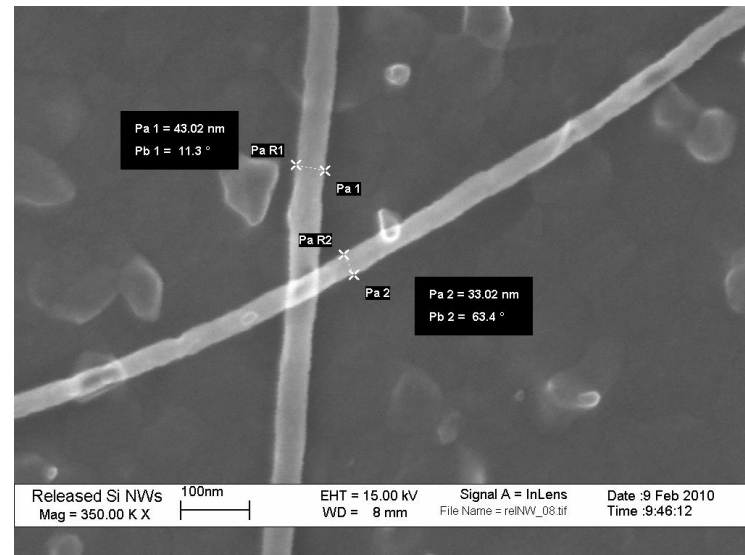
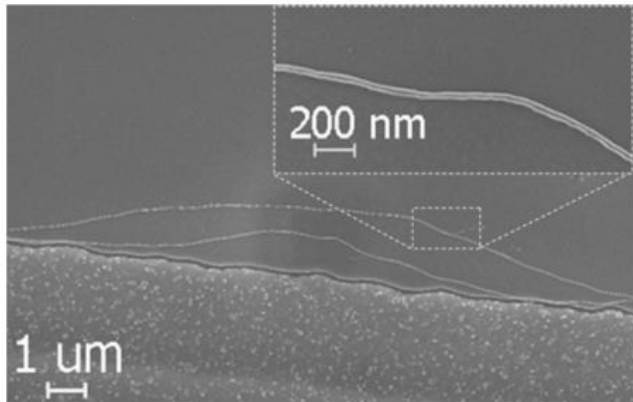
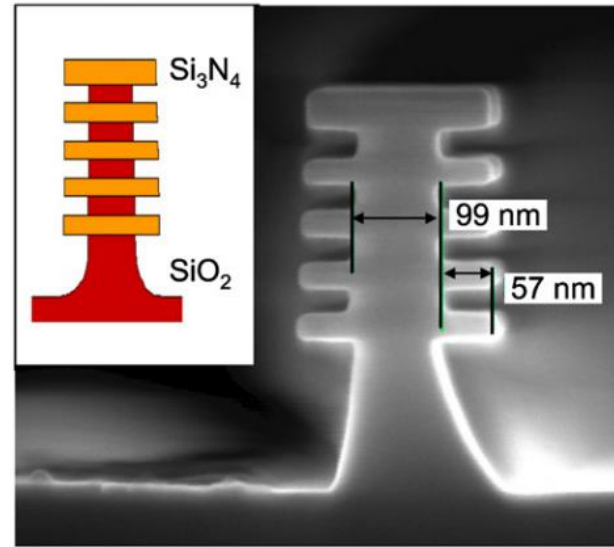
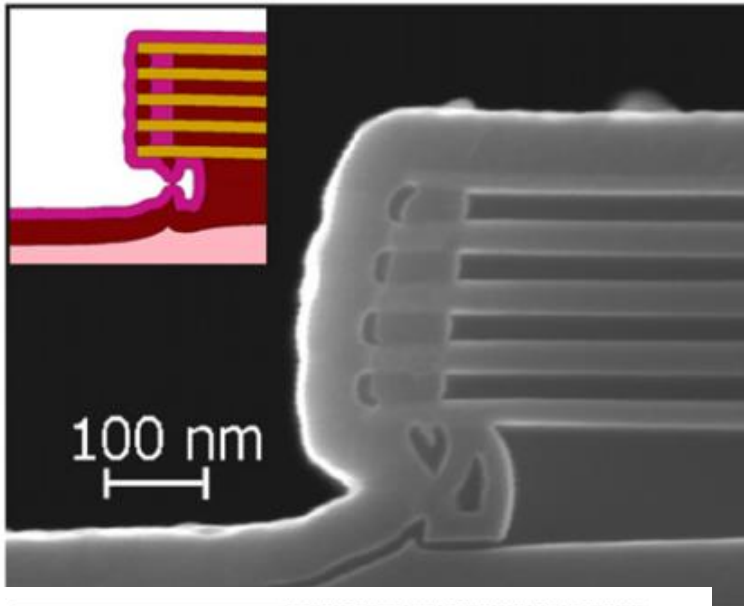
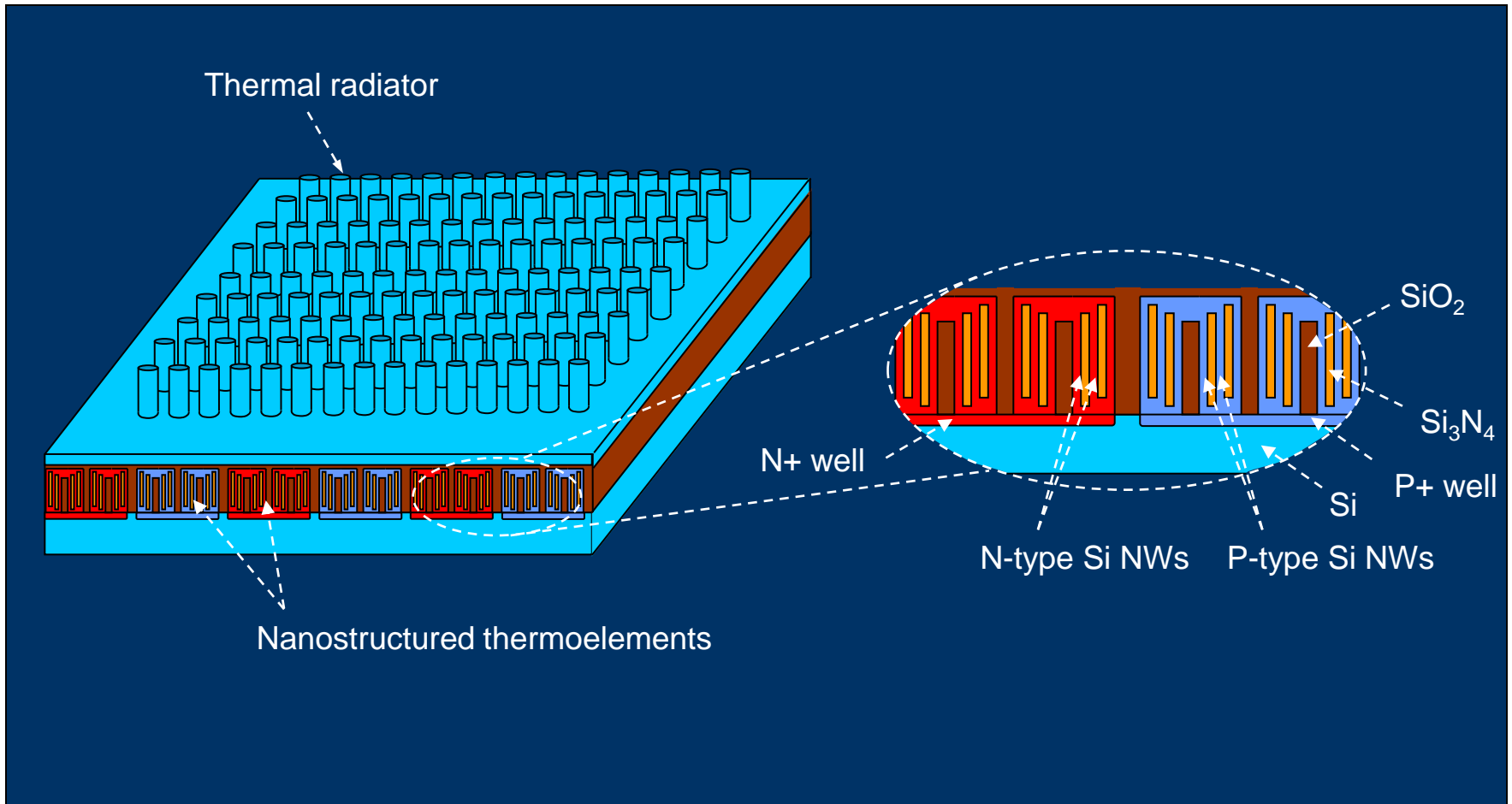


Fig. 5. SEM images at different magnifications of the nanowire after detachment from the hosting structure.

# Top-down layout with vertical NWs:



## From aims to practice

- NWs have high  $R_{th}$  ( $\approx 10^6 \text{ K W}^{-1}\text{nm}^{-1} / \text{NW}$ )
- For  $\Delta T = 50 \text{ K}$ , max heat acceptance is  $\approx 25 \text{ pW/NW}$   
@ wire length of 1 mm
- If  $\eta = 5 \%$  a target power output of  $10 \text{ }\mu\text{W/cm}^2$   
requires a wire density of  $10^8 \text{ cm}^{-2}$ , i.e. a wire spacing  
of about  $1 \text{ }\mu\text{m}$

## From aims to practice

Critical design issues are:

- optimal wire length
- optimal geometry (lateral or vertical)

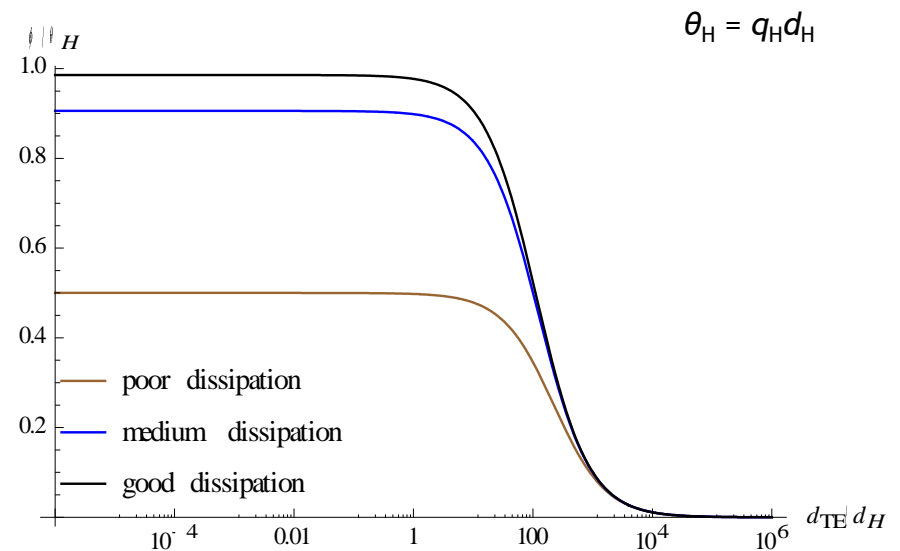
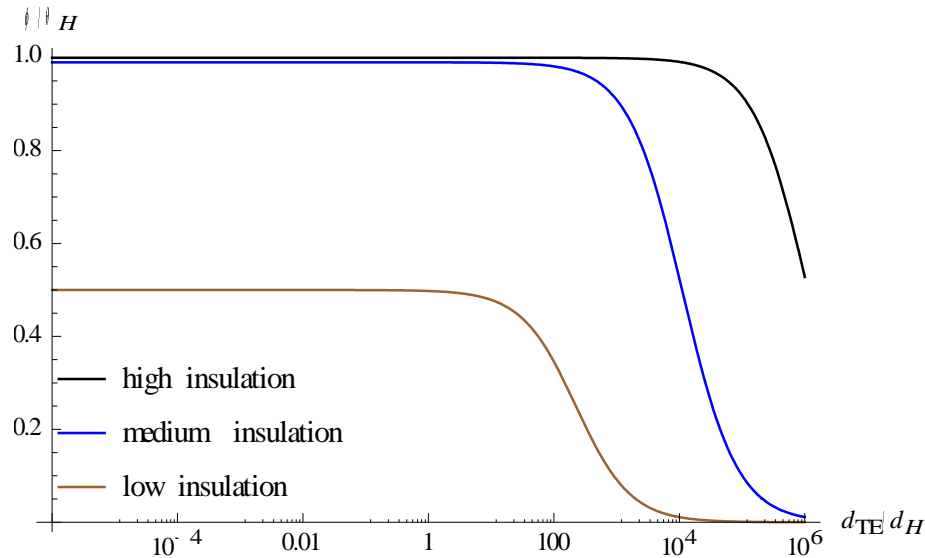
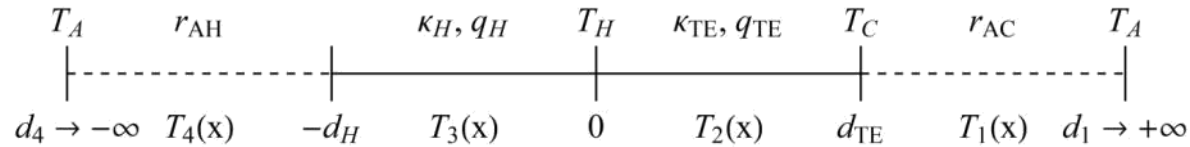
## TEG modeling

Choice of boundary conditions leads to contrasting design indications:

$$W_{el} = W_{th} \eta_{TE} = (\Delta T / R_{th}) \eta_{TE}$$

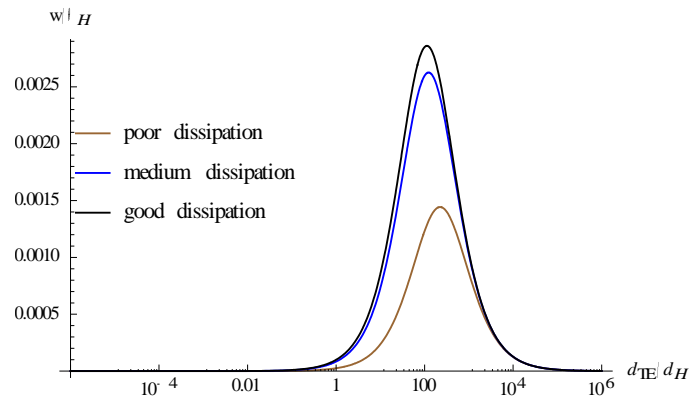
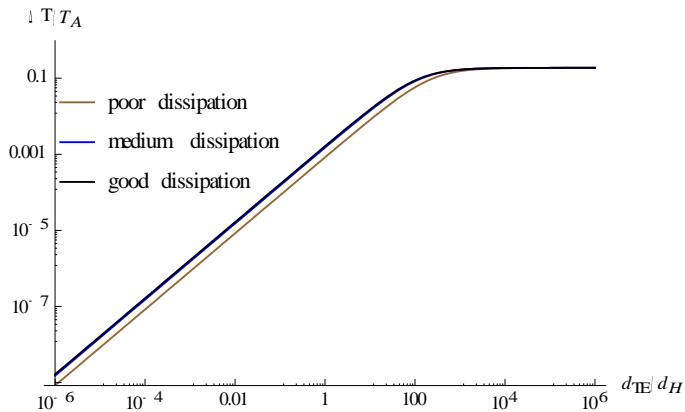
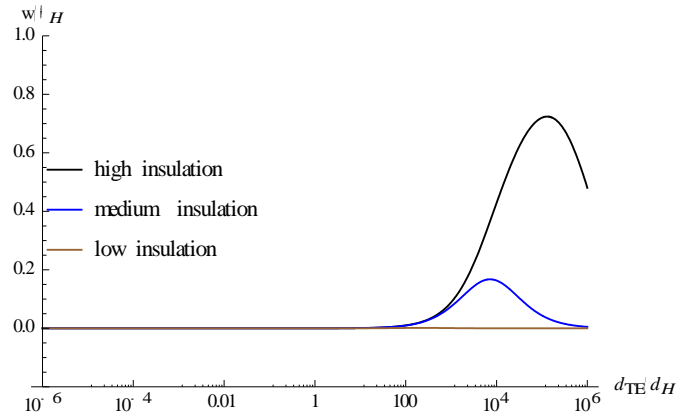
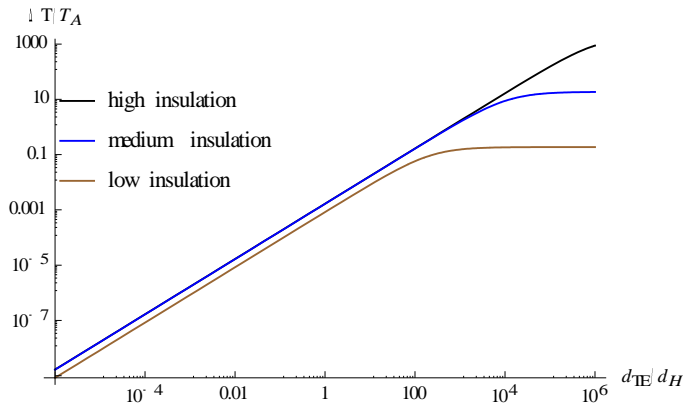
- setting fixed-T b.c.s:  $W_{el}$  increases as  $R_{th}$  decreases
- setting fixed-heatflow b.c.s:  $W_{el}$  increases as  $R_{th}$  increases

# TEG modeling

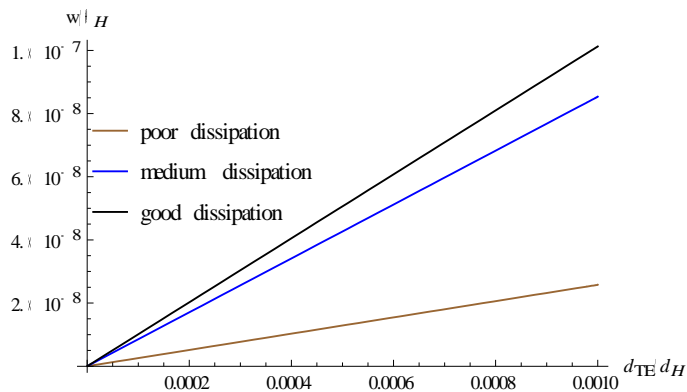
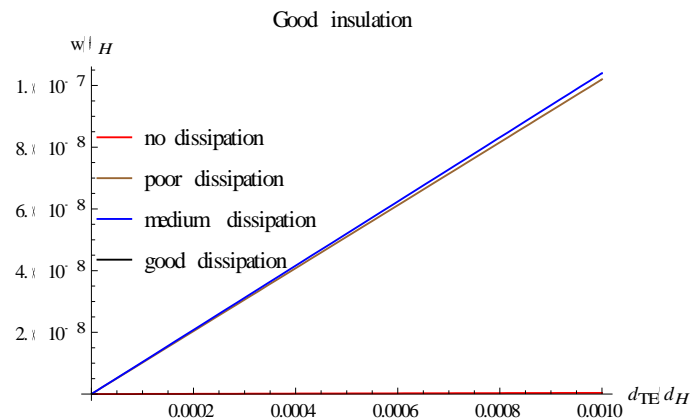
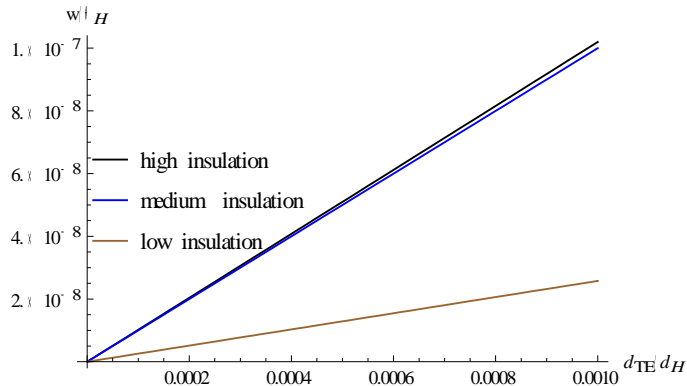




# TEG modeling



# TEG modeling



Thus:

- longer nanowires raise power output
- effective dissipation is relevant for poorly insulated heat sources

## Heat administration

TEGs will be mounted into a proper package that will deliver heat:

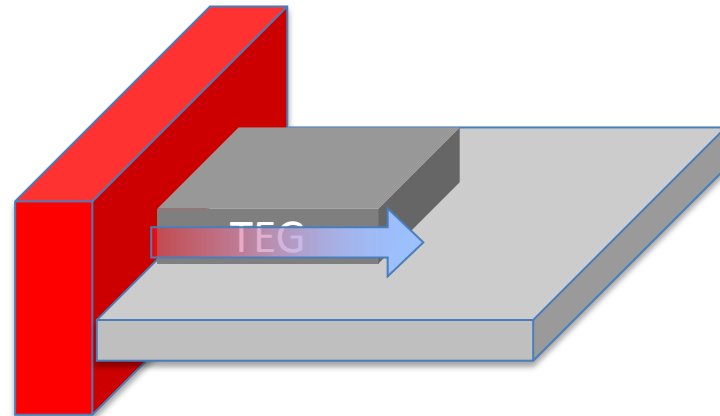
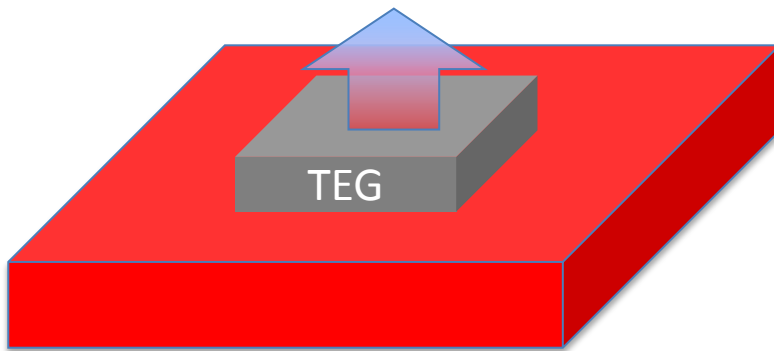
heat source → TEG → cold sink → ambient

- Higher heat radiator efficiency if series thermal resistances are small
- Parallel (shunt) resistance must be minimized

Both requirements are better satisfied if TEG geometry simplifies package design

## Heat direction

Two geometries (three layouts) addressed as of the 1st TEG generation



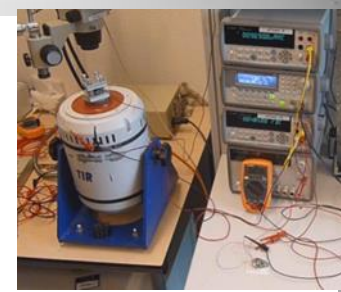
# Mechanical harvesters



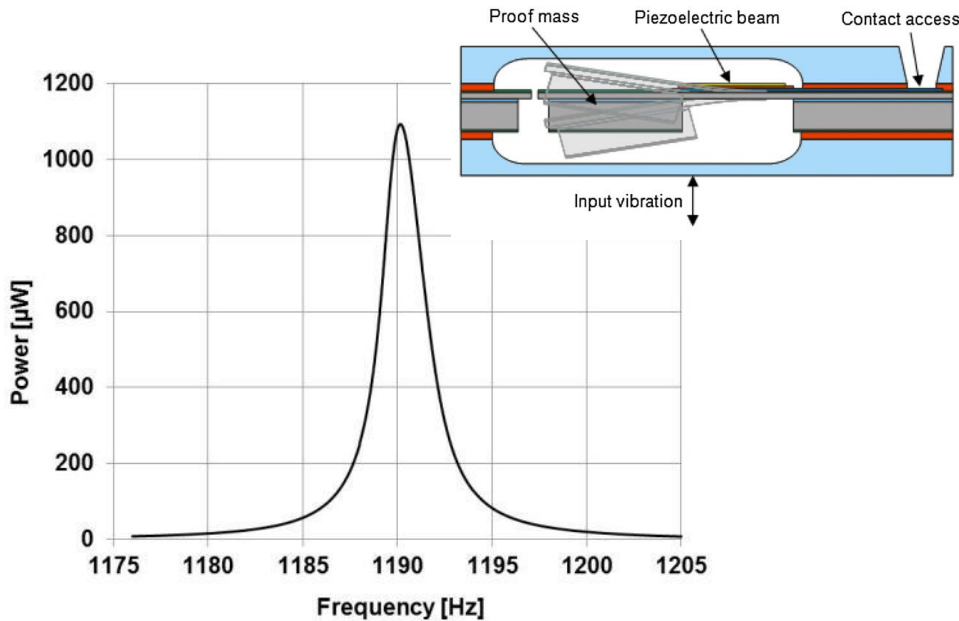


## Tire pressure monitoring system (TPMS)

- Today
  - Battery powered
  - Rim or valve mounted
- Battery replacement costs and effort
  - Energy harvester + system on the tire
    - Tire temperature
    - Tire identification

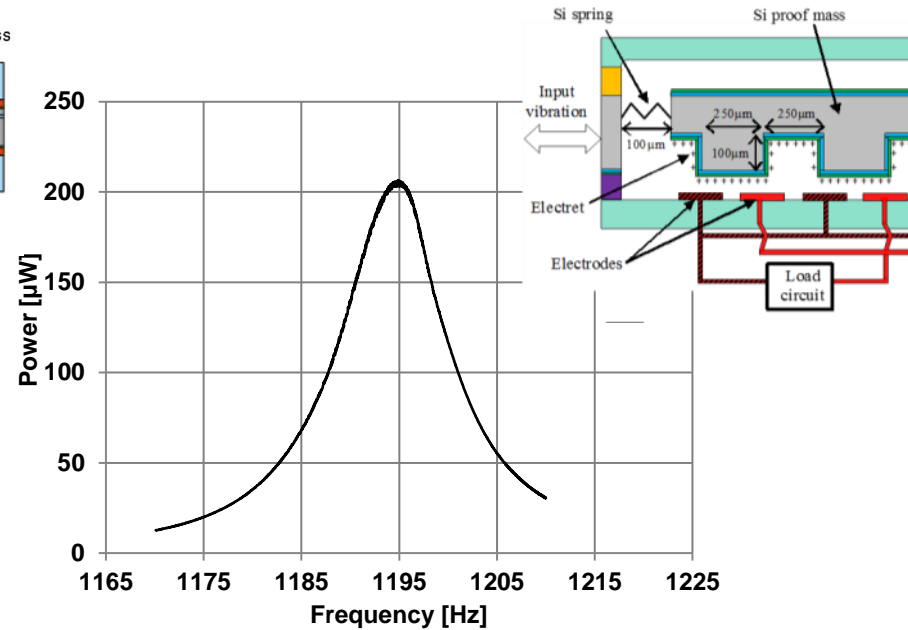


## Piezo



- Power output of 1100 $\mu\text{W}$
- Quality factor Q : 530
- Bandwidth BW : 2.3Hz
- Sensitivity : 262  $\mu\text{W}/\text{g}^2$

## Electrostatic

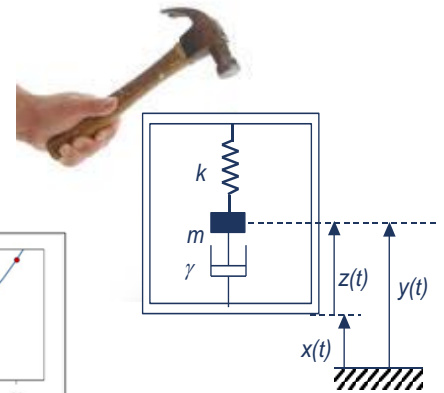


- Power output  $\sim 200\mu\text{W}$
- Quality factor Q : 93
- Bandwidth BW : 12.8 Hz
- Sensitivity : 130  $\mu\text{W}/\text{g}^2$

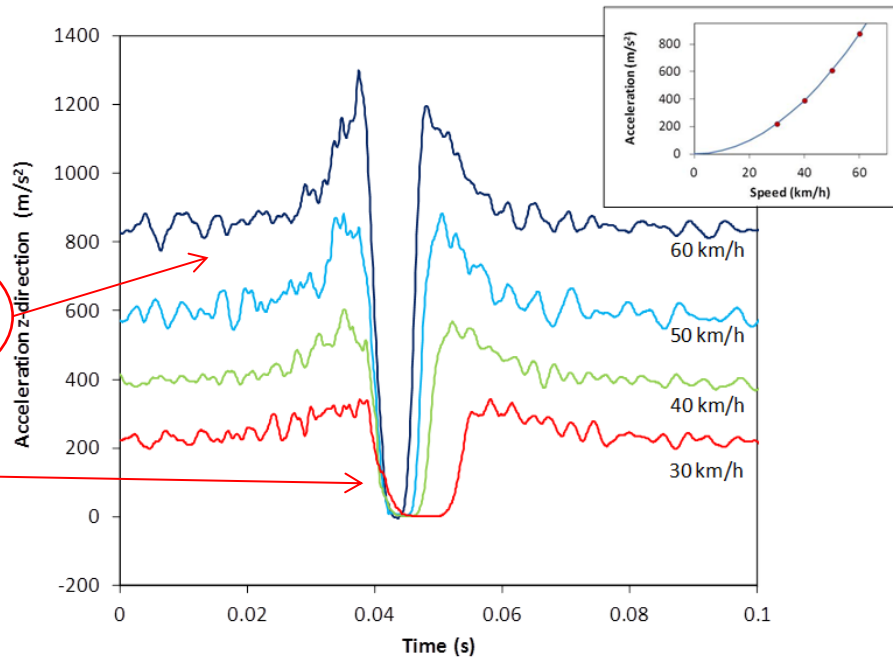
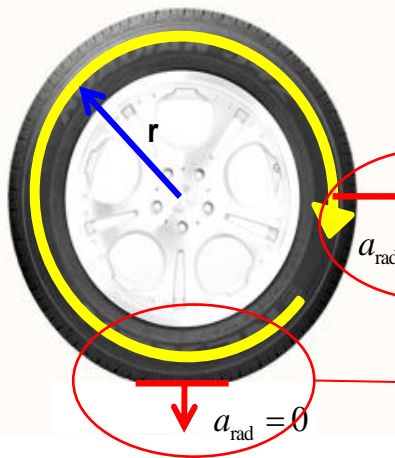


- Shock excitation inside tire
  - Power generation by shock excitation
  - Large shock available inside tire
  - Up to  $100\mu\text{W}$  @  $100\text{km/h}$  is feasible

Velocity damped resonator



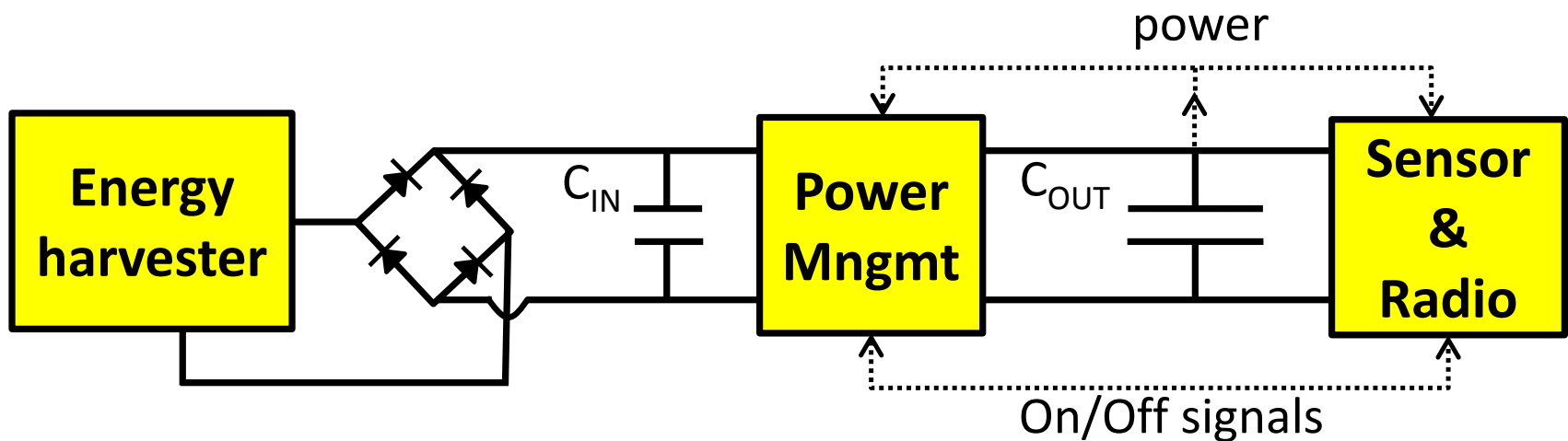
Energy generation inside tire



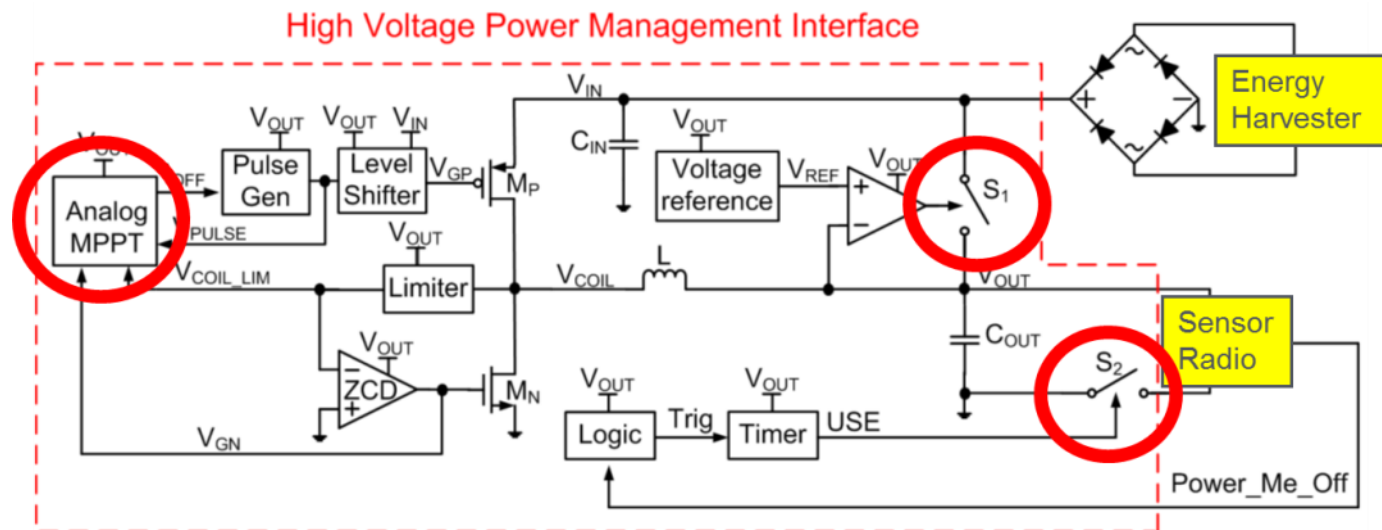
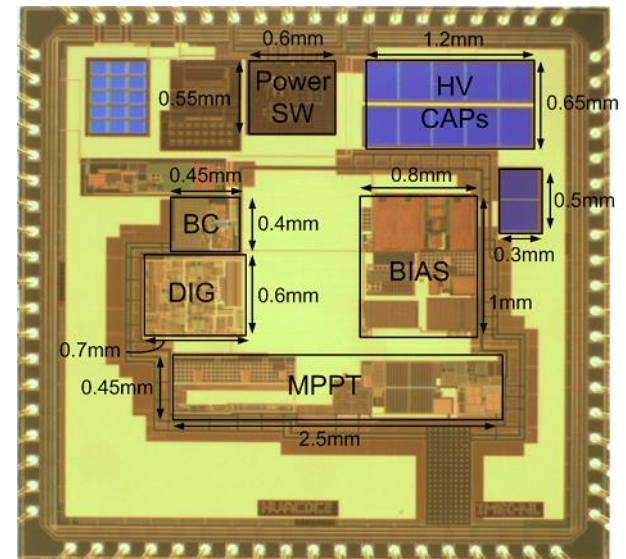


## Power generation is discontinuous

- Schematic system architecture



- Power Management
  - High voltage
  - 2 switches
  - Maximum Power Point Tracking
  - start-up from zero
  - $\eta=88\%$  at low power
  - $V_{out} \sim 2.5 V_{DC}$

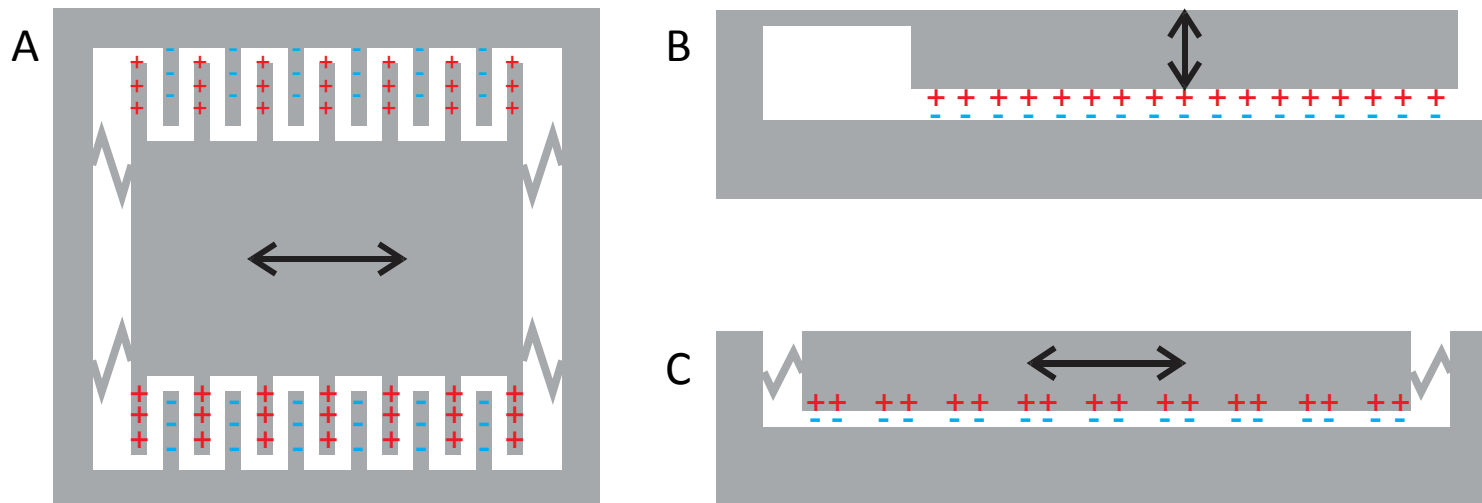


## Electrostatic energy harvesters

What do we need?

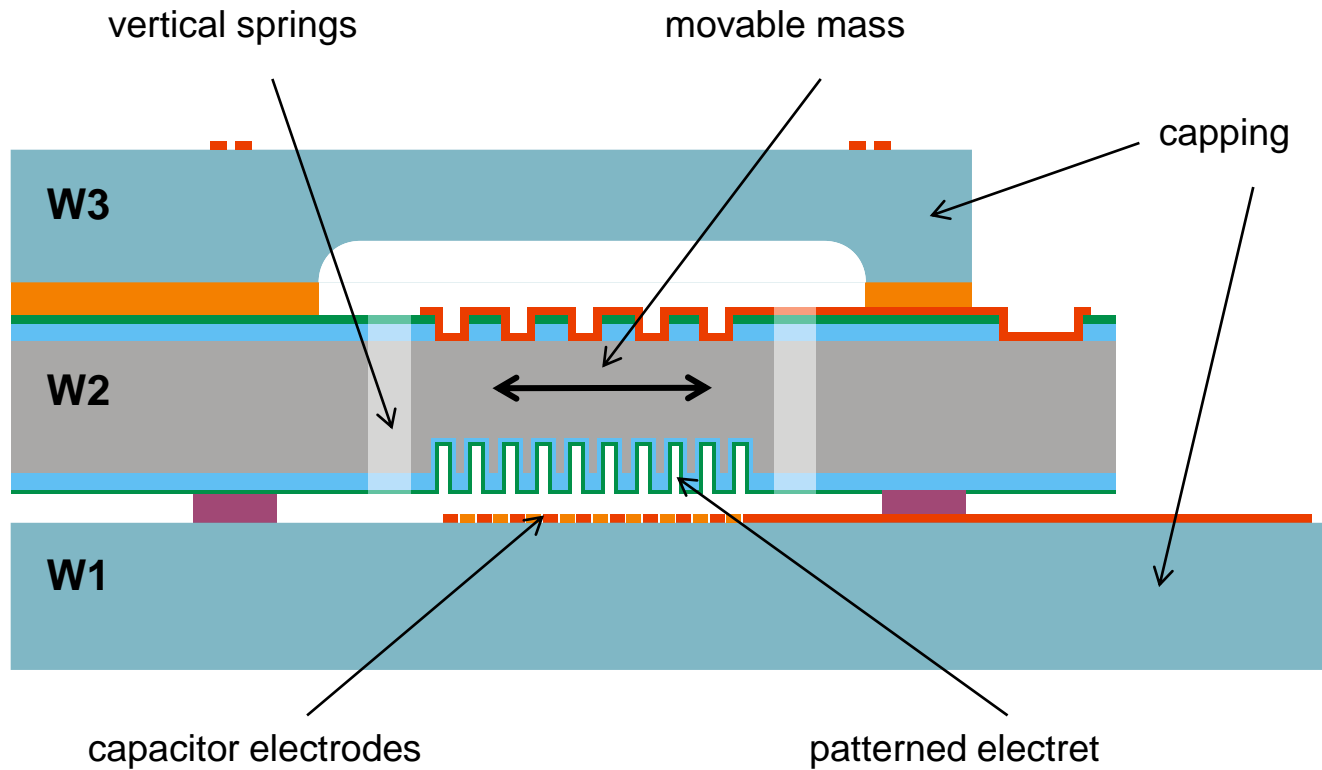
- **Vibrating mass**
  - Mass
  - Flexible springs
- **Variable capacitor**
  - Polarization source - charged electret
  - Electrodes
- **Packaging**
  - Capping

- Different operation principles possible

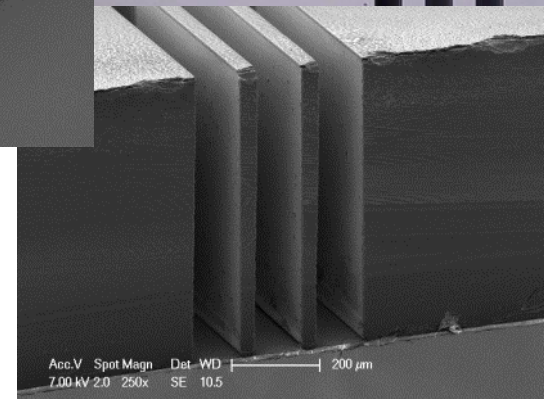
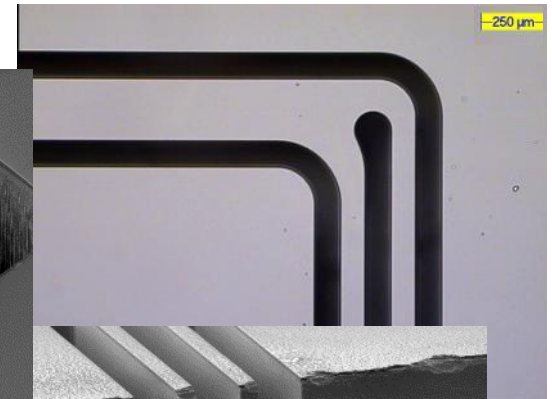
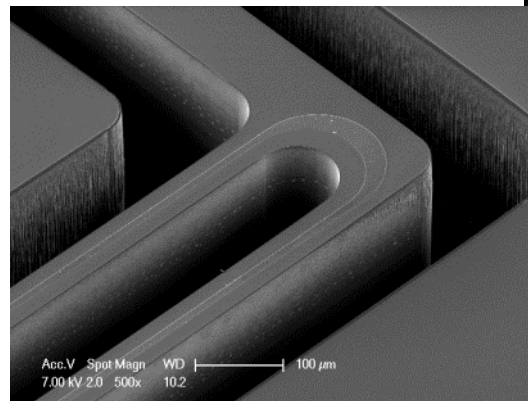
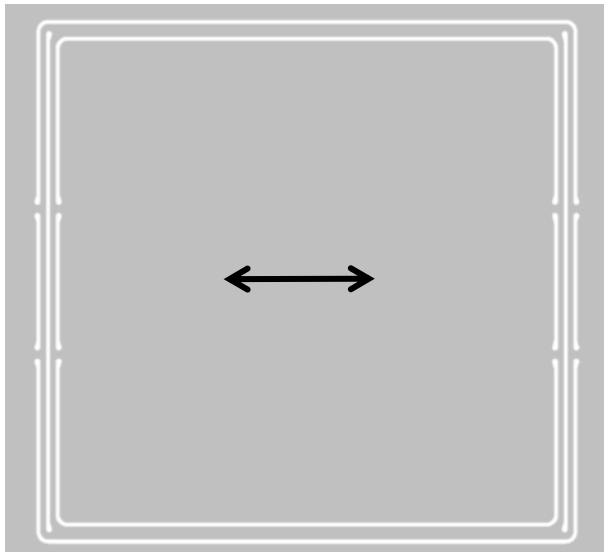


- A) in-plane gap closing
- B) Out-of-plane gap closing
- C) In-plane sliding capacitor

- In-plane sliding capacitor



- Device layout – mass/springs system
  - 1 cm<sup>2</sup> mass, full wafer thickness (650 μm)
  - 80μm thin springs, full wafer height
  - 100μm etched trenches, 100μm max mass amplitude

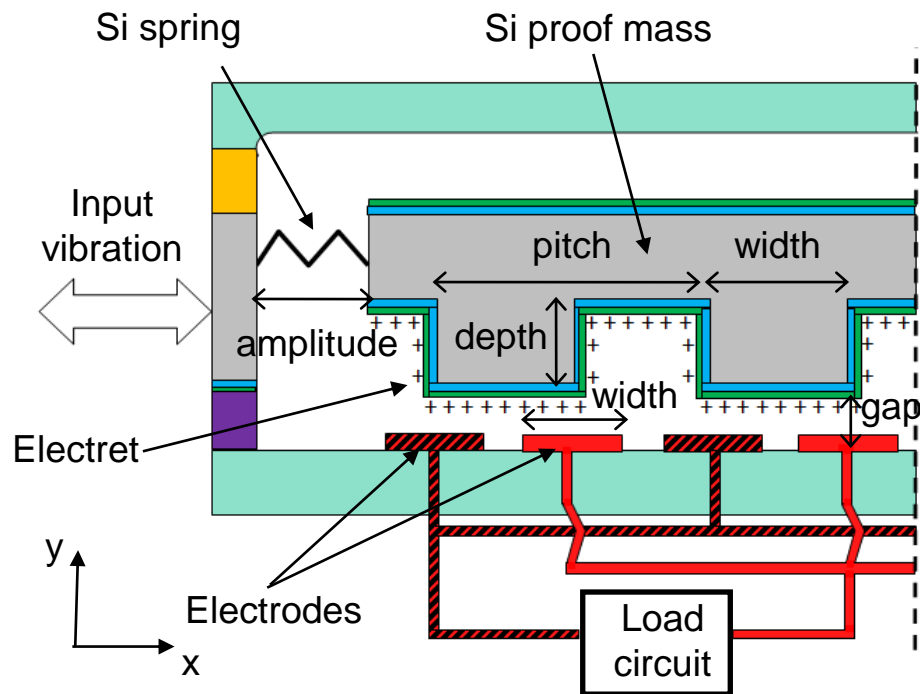


- **Materials – Electret**
  - Polymers (PVDF, BCB, Cytop) - low temperature stability
  - Inorganic materials ( $\text{SiO}_2$ ,  $\text{Si}_3\text{N}_4$ ) - CMOS compatible deposition
- **Interface  $\text{SiO}_2$ - $\text{Si}_3\text{N}_4$  can trap stable charges**
- **Parameters to play with:**
  - Oxide Thickness
  - Nitride Thickness
  - Material quality (deposition method)
  - Multilayers
  - Charge patterning method

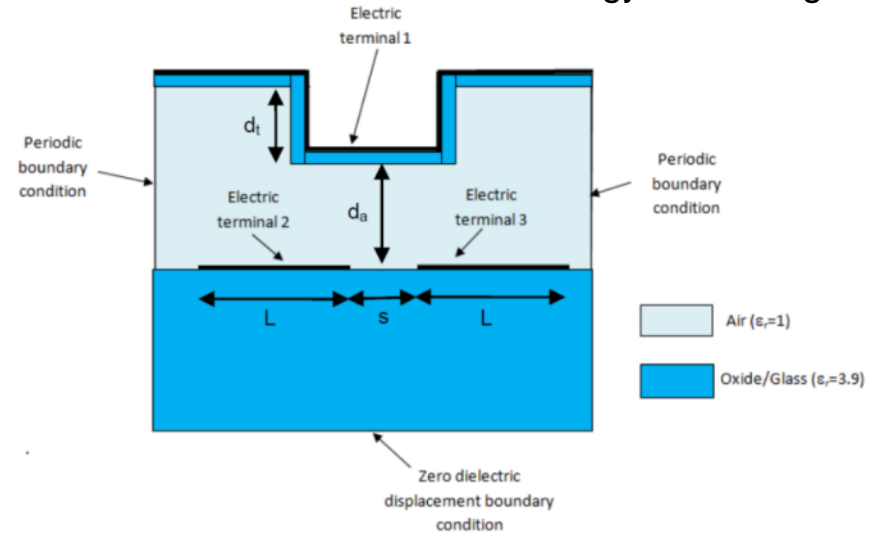
- Electret layer – results and choices
- SiO<sub>2</sub> thickness:
  - 500nm - charge decay
  - 2000nm - no charge separation after RTA
  - 1000nm - good
- Si<sub>3</sub>N<sub>4</sub> thickness:
  - Little influence, 150nm - good
- Deposition method:
  - Thermal oxide + LPCVD Si<sub>3</sub>N<sub>4</sub> - good
  - TEOS, PECVD oxide and nitride - charge decay
- Multilayers: no extra charge



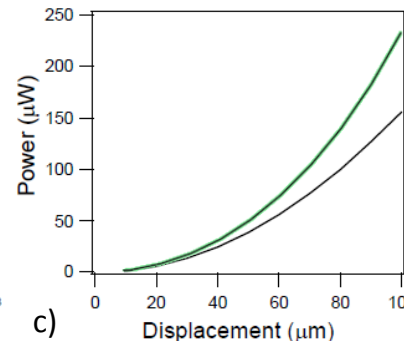
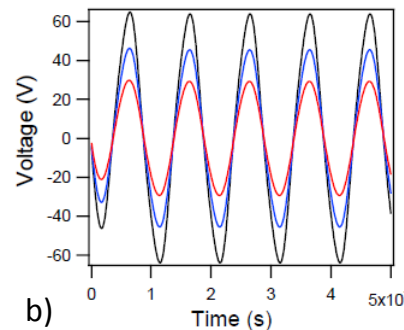
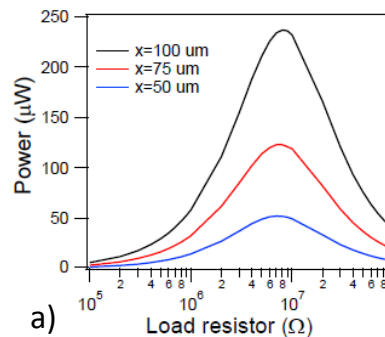
- Device layout – electret / electrode configuration



- Device layout – optimization
  - Finite element modelling



- Typical modelling result

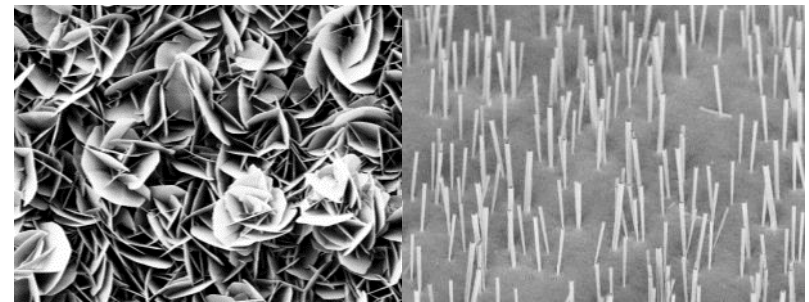
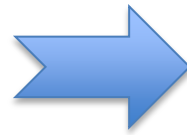
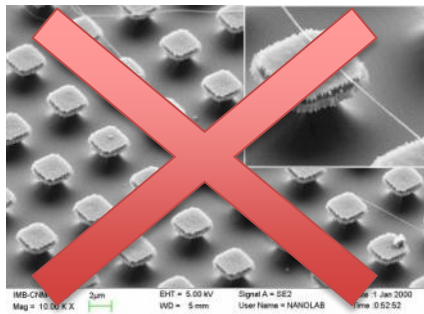


Corrugated electret  
VS  
Planar electret

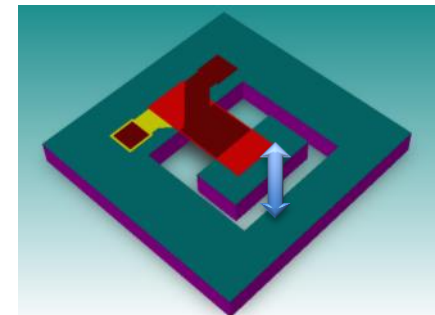
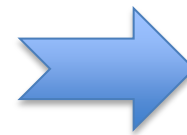
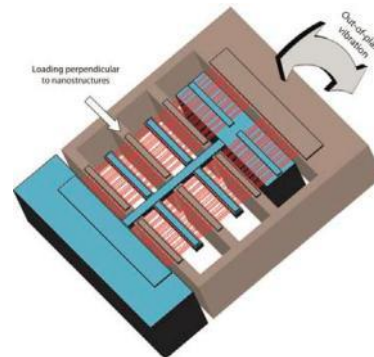
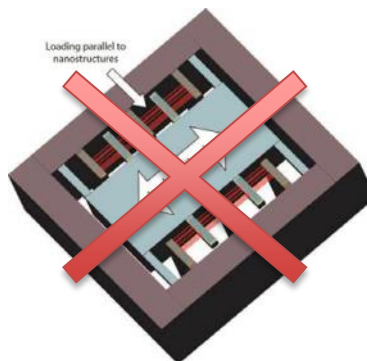
- Predicted maximum output power: 500μW
  - 1kHz 2.5G sinusoidal input vibration (resonance), full 100μm mass displacement

## Piezoelectric harvesting

New approach uses ZnO nanowires (NWs) and nanosheets (NSs)  
 Standard AlN thin-film approach will be used as a benchmark

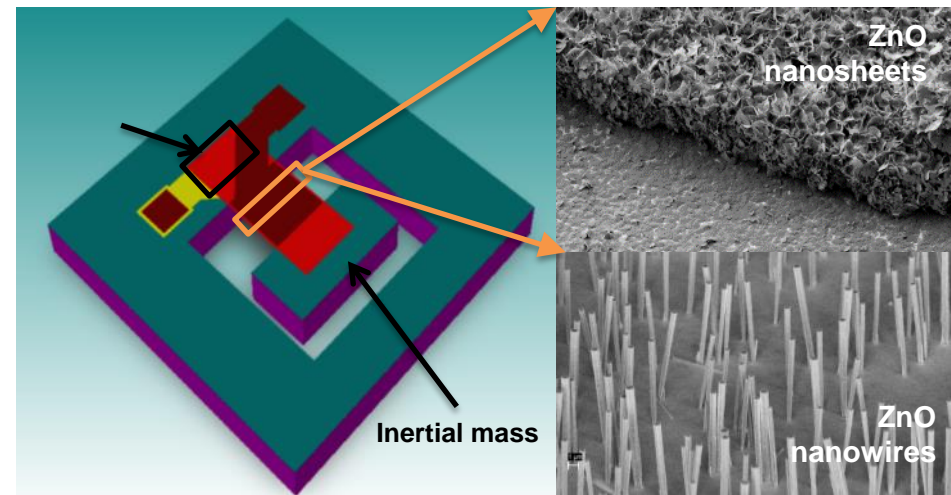


ZnO nanowires are much easier to grow and integrate with silicon  
 ZnO NW & NS growth is also a low-cost solution and a hot-topic

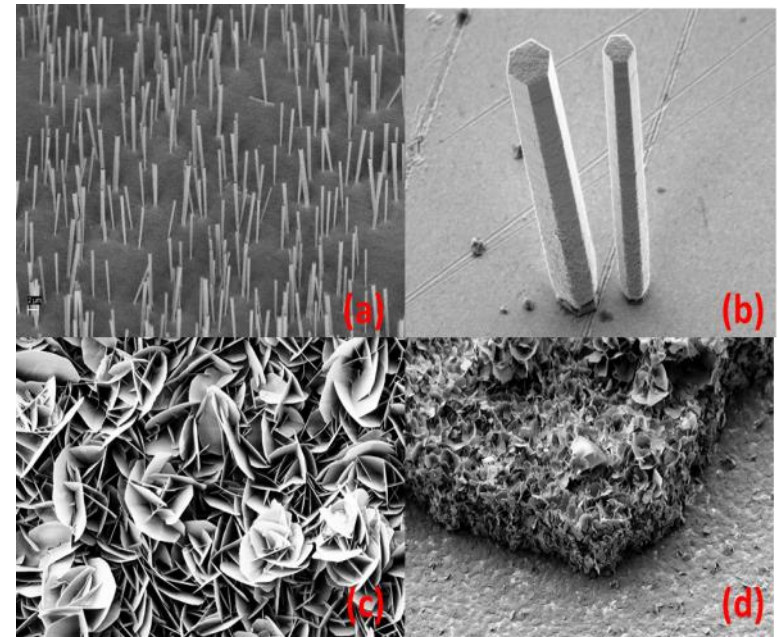


## What do we need?

- Inertial mass & cantilevered spring
  - Mass
  - Flexible spring
- Piezoelectric material
  - ZnO nanowires & nanosheets
  - AlN thin-film (for benchmark)
  - Electrodes

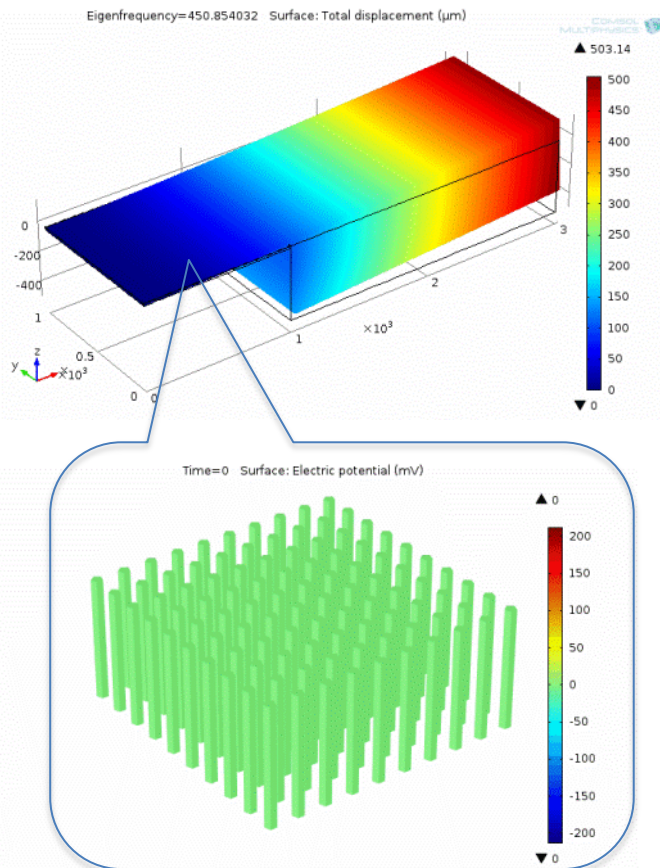


- **New piezoelectric materials**
  - ZnO nanostructures will be used as **replacement of original approach** based on nanofibres:
    - ZnO nanowires .
    - ZnO nanosheets .
  - More mature technology compared to nanofibres that needs a more important technology development
  - **Inherent piezoelectric behavior of ZnO**
  - Easier to integrate with silicon
  - **High novelty provided by ZnO nanosheets**

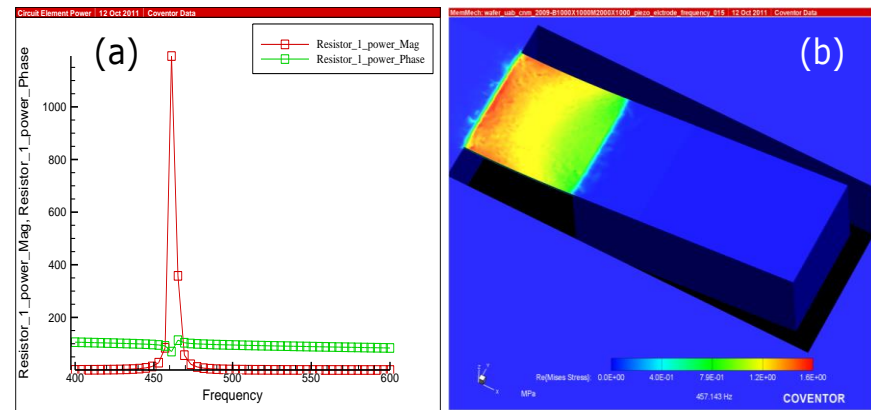


*ZnO nanowires (overall view (a) and detailed view (b)), and nanosheets (top view (c) and tilted view (d)). NW lengths range from 2 to 5  $\mu\text{m}$  and thicknesses from 100 nm to 900 nm.*

# Predicted output power



For FEM simulations a **power density of  $47 \mu\text{W}/\text{cm}^2$**  at 447 Hz ( $Q = 50$ ) for 1 g has been calculated. An expected power density of around  **$400 \mu\text{W}/\text{cm}^2$**  for an acceleration of 10 g is a **good target**.

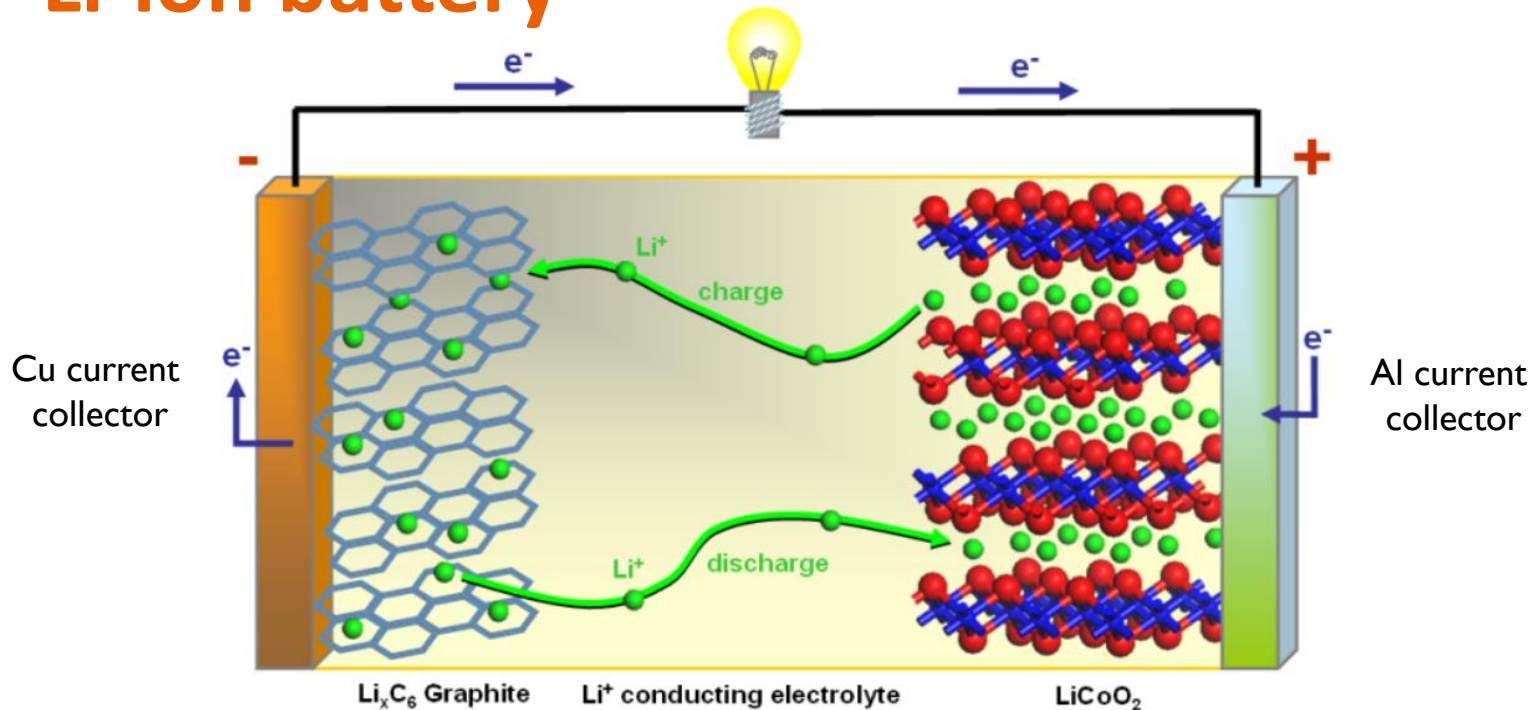


Generated power (in nW) and main stress in the structure when it is bent

# Batteries



# Li-ion battery



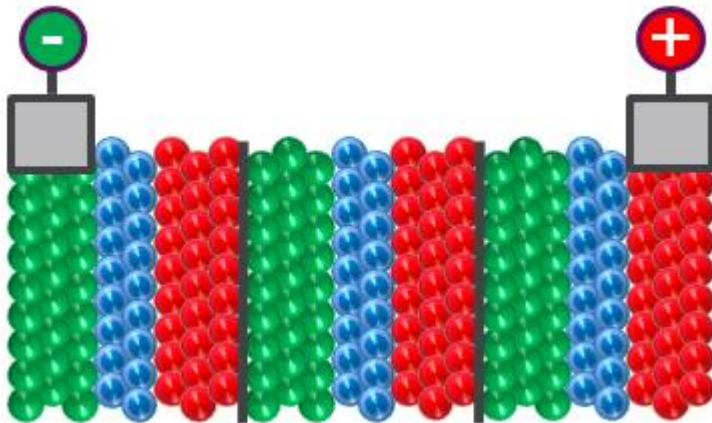
## Charge and discharge process of an Li-ion battery

During charging  $\text{Li}^+$  ions are liberated from the cathode and transported through the liquid electrolyte to the anode, where the  $\text{Li}^+$  is reduced by the electrons coming from the electrical circuit.



## THICK BATTERIES

kWh - Wh

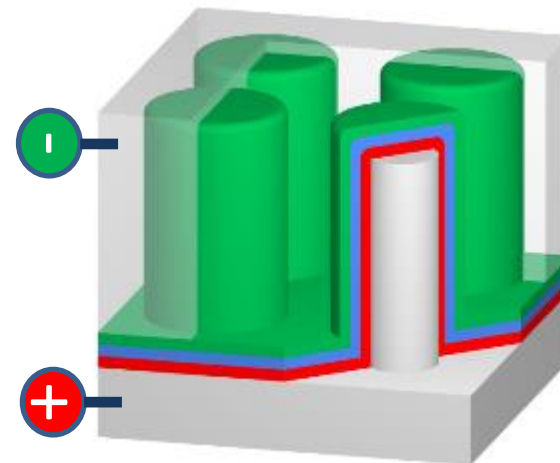


**High capacity devices with competitive power**

- *Pressed pellets/bipolar stacks*
- *Solid electrolytes with high  $\sigma_{ionic}$*
- *Low-impedance interfaces*

## THIN-FILM BATTERIES

Wh - mWh

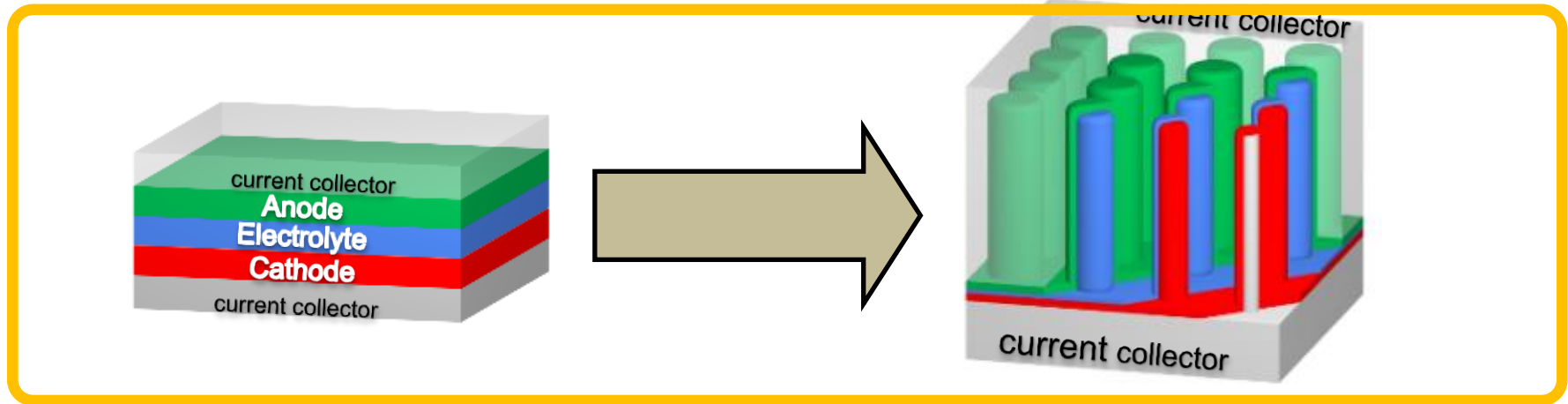


**High-power devices with competitive capacity**

- *Film thickness scaling*
- *3D surface area enhancement*
- *Process up-scaling/large area foils*



## Fabrication of functional thin-film micro-battery for integrated storage



Planar thin-film device

3D thin-film battery

*Lattice matched spinel stack*

*Si compatible fabrication process*

*Electrolyte and interface engineering for power (charging rate)*

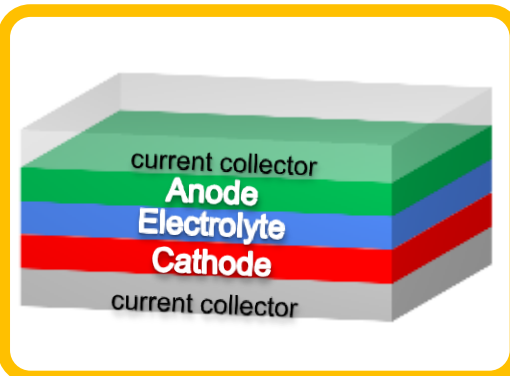
*Micro-structured architectures for increased battery capacity and power (current)*

*0.05 mAh/cm<sup>2</sup> at 0.1C, and 60% capacity at 10C (1 mA/cm<sup>2</sup>)*

*0.5mAh/cm<sup>2</sup> at 0.1C, and 50% capacity at 5C rate (2.5 mA/cm<sup>2</sup>)*

# Standard planar micro-battery integration

One interface at a time approach



Current collector

*TiN, Pt, SiC, TiC, Cu*

$Li_4Ti_5O_{12}$  **Anode** (1.55V vs.  $Li^+/Li$ )

- Negligible volume expansion
- Spinel structure
- Capacity: 610mAh/cm<sup>3</sup>

$Li_4Ti_5O_{12}$   
 $TiO_2$   
*a-Si*

Solid State Electrolyte Requirements

1. Pinhole-free
2. High ionic conductance ( $\sigma_i > 10^{-5} S$ )
3. Electrochemical window (0.5 < V vs.  $Li^+/Li$  < 4.5)
4. Chemical stability (electrodes, Li)
5. Small electronic conductivity ( $\sigma_e < 10^{-10} S/cm$ )

$LiAlO_2$   
 $Li_4SiO_4$   
 $Li_5AlSi_2O_3$   
 $LiMgTiO_3$   
 $LiTaO_3$   
 $Li_xMg_{1-2x}Al_{2+x}O_4$   
 $Li_{3x}La_{(2/3)}\square_{x(1/3)-2x}TiO_3$

$LiMn_2O_4$  **Cathode** (4.0V vs.  $Li^+/Li$ )

- low cost, low toxicity and abundant
- Spinel structure
- Capacity: 650mAh/cm<sup>3</sup>

$LiMn_2O_4$   
 $MnO_2$

Current collector

*TiN, Pt, SiC, TiC, Al*

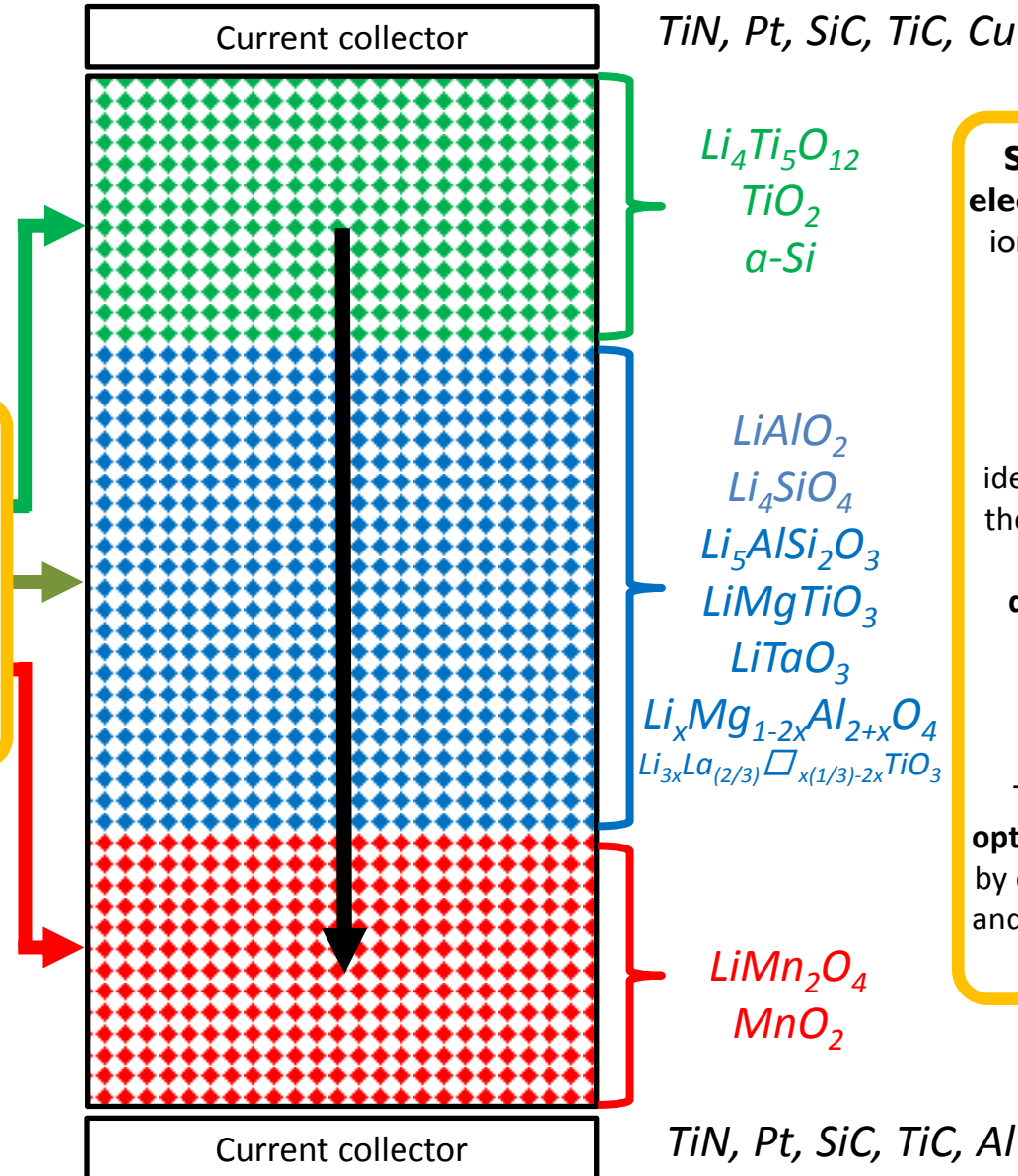
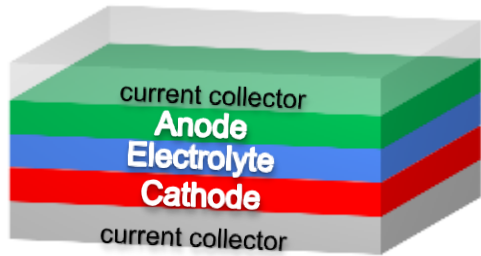
**Compatible material stack:**  
Diffusion barrier, seed, CMOS processes, thermal budget compatibility

**Feasibility** of post-deposition lithiation schemes of CMOS compatible stacks

**Suitable solid/spinel electrolyte composition:**  
ionic conductivity versus stability

# Enhanced micro-battery integration

Transparent interfaces *all-spinel* battery stack matching crystal lattice



**Suitable solid/spinel electrolyte composition:**  
ionic conductivity versus stability

A suitable spinel electrolyte will be identified by **screening** of the composition with the aid of **combinatorial deposition in the PLD** system (4 targets)

The **interfaces** will be **optimized** for ionic transfer by compositional gradients and interfacial buffer layers

## Fabrication of on-chip thin-film micro-batteries

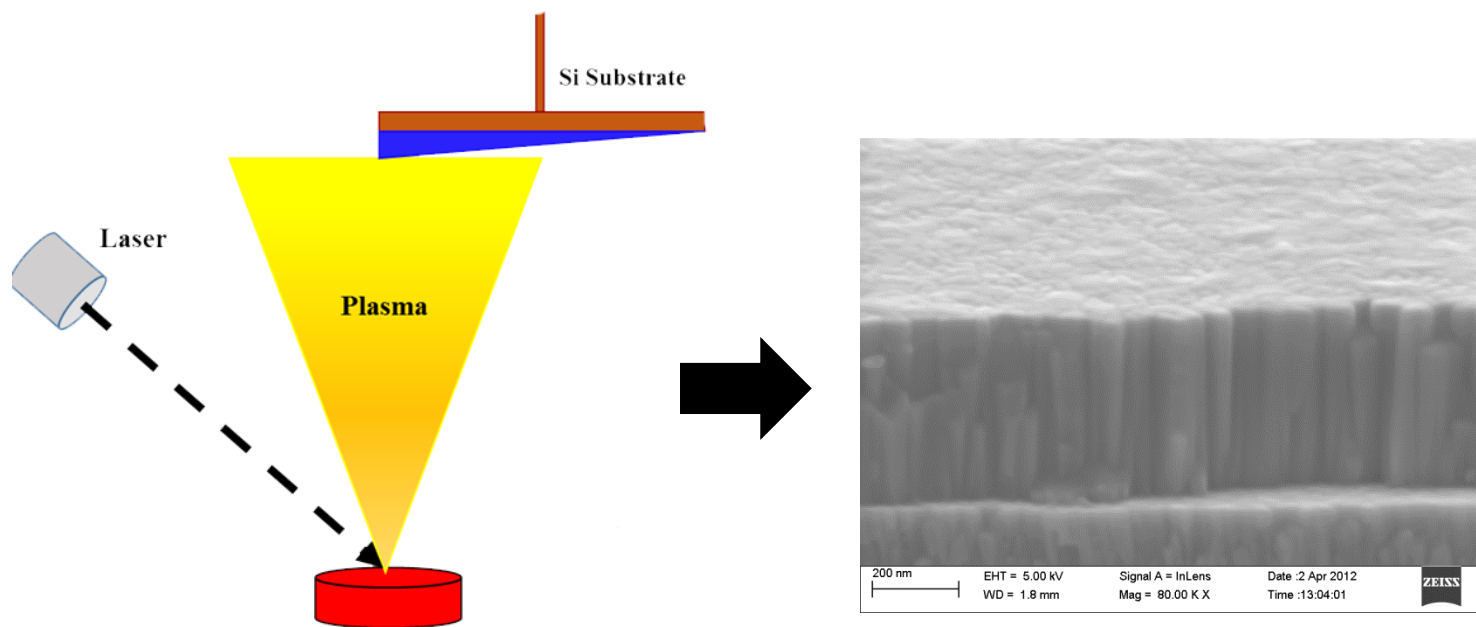
**PLD deposition technique. Three approaches:**

- Single layer
- Multilayer
- Combinatorial

**Optimization of thin film deposition**

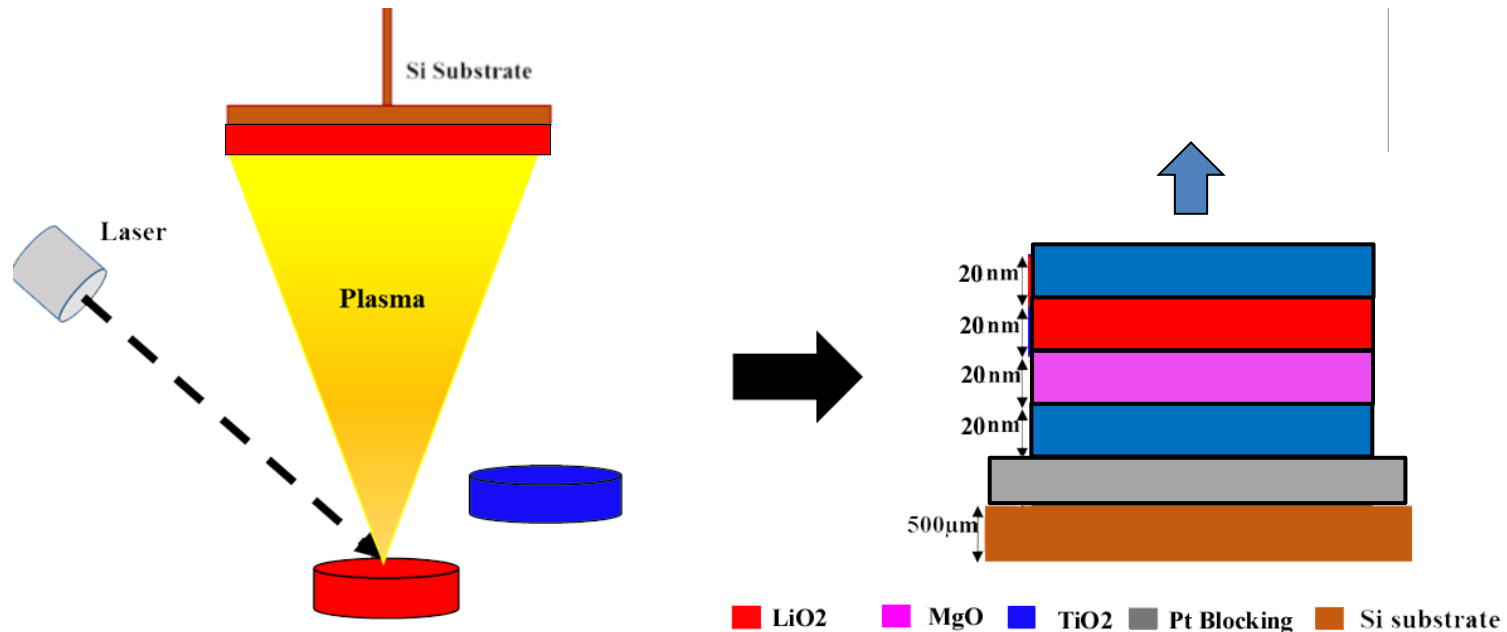
- Single target deposition:
  - $\text{TiO}_2$
  - $\text{Li}_2\text{O}$
  - $\text{MgO}$
- Stacking of single layers: formation of **complex oxides**

## PLD deposition: single layer deposition



- Possibility of generating dense thin ceramic layers
- Good reproducibility of target stoichiometry
- Possibility of layer microstructure control (P, T, Laser energy...)

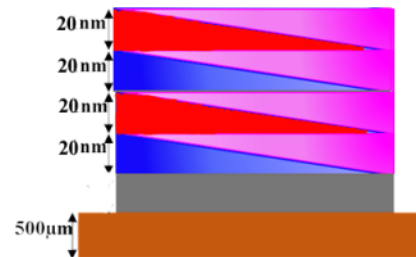
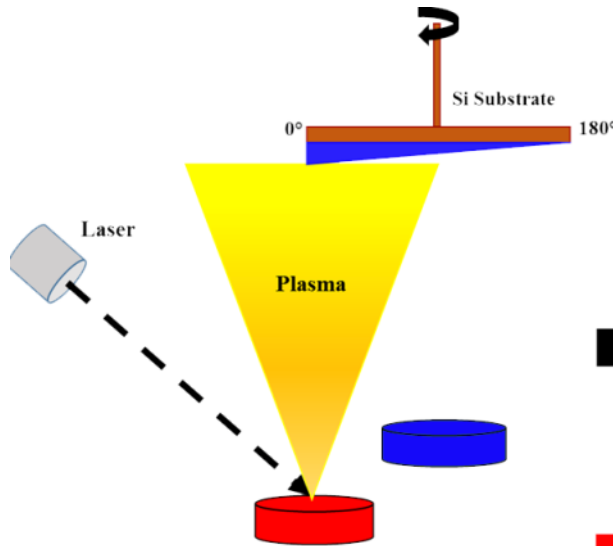
## PLD deposition: Multi-layer deposition



Choosing right deposition parameters it is possible to:

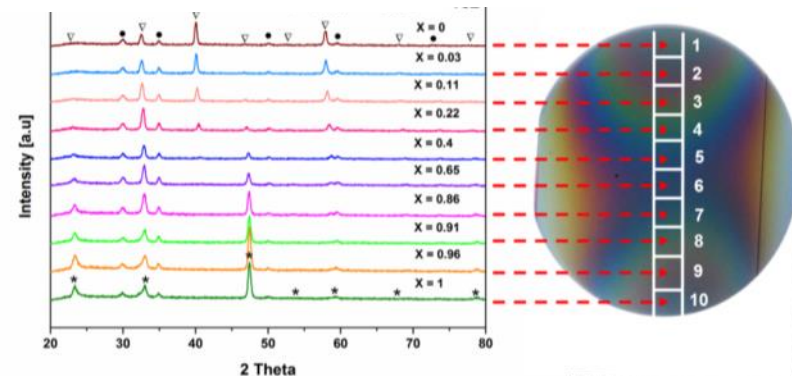
- Deposit multi-layers with good quality interfaces or
- Generate a complex material by thermal diffusion.

# PLD deposition: combinatorial approach



■ LiO<sub>2</sub>   
 ■ MgO   
 ■ TiO<sub>2</sub>   
 ■ Pt Blocking   
 ■ Si substrate

- Large area system allows producing a combinatorial sample
- A full mapping of material composition can be generated in one shot



NIMP3-SL-ZU13-0U4109



# Summary & Outlook



## Summary

- All-silicon harvester found feasible
- Delivered power expected to fulfill diverse WSN specs
- Solutions are cost-effective and do not require non-standard-IC processing

## The Team

Luis Fonseca (CSIC, Project leader)

CSIC: Carlos Calaza, Marc Salleras, Jaume Esteve, Gonzalo Murillo, Carlos Camargo

Confindustria: Danilo Mascolo, Annamaria Raimondi, L. Rossi

Electrolux: Claudio Cenedese

IREC: Albert Tarancon, Alex Morata, M. Torrell, G. Gadea, J.D. Santos, M. Fehse

IMEC (Belgium): Philippe Vereecken, Cedric Huyghebaert, Brecht Put, Maarten Mees, Alfonso Sepulveda Marquez

IMEC (Netherlands): Rob Van Schaijkl, Martijn Goedbloed

STE: Paolo Moiraghi, Mauro Cortese

U. of Milano Bicocca: Dario Narducci, Laura Zulian

IMM-CNR: Alberto Roncaglia, Fulvio Mancarella



[sinergy-project.eu](http://sinergy-project.eu)

Contact: [luis.fonseca@imb-cnm.csic.es](mailto:luis.fonseca@imb-cnm.csic.es)

*This work was supported by FP7-NMP-2013-SMALL-7, SiNERGY (Silicon Friendly Materials and Device Solutions for Microenergy Applications), Contract n. 604169*



[sinergy-project.eu](http://sinergy-project.eu)  
Contact: [luis.fonseca@imb-cnm.csic.es](mailto:luis.fonseca@imb-cnm.csic.es)